Accepted Manuscript

Discovery of Polar Spirocyclic Orally Bioavailable Urea Inhibitors of Soluble Epoxide Hydrolase

Alexey Lukin, Jan Kramer, Markus Hartmann, Lilia Weizel, Victor Hernandez-Olmos, Konstantin Falahati, Irene Burghardt, Natalia Kalinchenkova, Darya Bagnyukova, Nikolay Zhurilo, Jarkko Rautio, Markus Forsberg, Jouni Ihalainen, Seppo Auriola, Jukka Leppänen, Igor Konstantinov, Denys Pogoryelov, Ewgenij Proschak, Dmitry Dar'in, Mikhail Krasavin
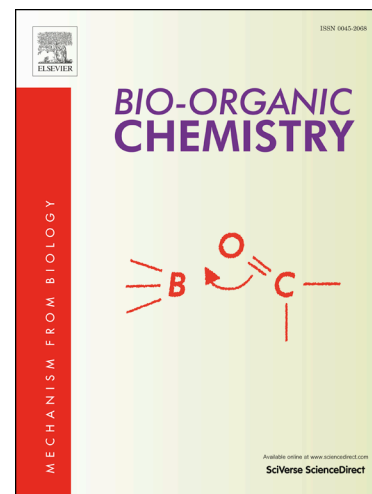
Please cite this article as: A. Lukin, J. Kramer, M. Hartmann, L. Weizel, V. Hernandez-Olmos, K. Falahati, I. Burghardt, N. Kalinchenkova, D. Bagnyukova, N. Zhurilo, J. Rautio, M. Forsberg, J. Ihalainen, S. Auriola, J. Leppänen, I. Konstantinov, D. Pogoryelov, E. Proschak, D. Dar'in, M. Krasavin, Discovery of Polar Spirocyclic Orally Bioavailable Urea Inhibitors of Soluble Epoxide Hydrolase, *Bioorganic Chemistry* (2018), doi: https://doi.org/10.1016/j.bioorg.2018.07.014

Discovery of Polar Spirocyclic Orally Bioavailable Urea Inhibitors of Soluble Epoxide Hydrolase

Alexey Lukin,[a] Jan Kramer,[b] Markus Hartmann,[b] Lilia Weizel,[b] Victor Hernandez-Olmos,[c] Konstantin Falahati,[d] Irene Burghardt,[c] Natalia Kalinchenkova,[a] Darya Bagnyukova,[a] Nikolay Zhurilo,[a] Jarkko Rautio,[e] Markus Forsberg,[e] Jouni Ihalainen,[e] Seppo Auriola,[e] Jukka Leppänen,[e] Igor Konstantinov,[f] Denys Pogoryelov,[g] Ewgenij Proschak,[b] Dmitry Dar'in[h] and Mikhail Krasavin[h,*]

[a]Lomonosov Institute of Fine Chemical Technologies, Moscow Technological University, Moscow 117571 Russian Federation

[b]Institute of Pharmaceutical Chemistry, Goethe University, Frankfurt, Max-von-Laue-Straße 9, 60438 Frankfurt, Germany

[c]Fraunhofer IME-TMP, Max-von-Laue-Straße 9, 60438 Frankfurt, Germany

[d]Institute of Physical and Theoretical Chemistry, Goethe University Frankfurt, Max-von-Laue-Straße 7, 60438 Frankfurt, Germany

[e]School of Pharmacy, University of Eastern Finland, 70211 Kuopio, Finland

[f]N. D. Zelinsky Institute of Organic Chemistry, 47 Leninsky prospect, Moscow, 119991, Russian Federation

[g]Institute of Biochemistry, Goethe University Frankfurt, Max-von-Laue-Straße 9, 60438 Frankfurt, Germany

[h]Saint Petersburg State University, Saint Petersburg 199034 Russian Federation

*Corresponding author. Tel.: +7 931 3617872; fax: +7 812 428 6939. E-mail address: m.krasavin@spbu.ru (M. Krasavin).

Abstract: Spirocyclic 1-oxa-9-azaspiro[5.5]undecan-4-amine scaffold was explored as a basis for the design of potential inhibitors of soluble epoxide hydrolase (sEH). Synthesis and testing of the initial SAR-probing library followed by biochemical testing against sEH allowed nominating a racemic lead compound **(±)-22**. The latter showed remarkable (> 0.5 mM) solubility in aqueous phosphate buffer solution, unusually low (for sEH inhibitors) lipophilicity as confirmed by experimentally determined $logD_{7.4}$ of 0.99, and an excellent oral bioavailability in mice (as well as other pharmacokinetic characteristics). Individual enantiomer profiling revealed that the

inhibitory potency primarily resided with the dextrorotatory eutomer **(+)-22** (IC$_{50}$ 4.99 ± 0.18 nM). For the latter, a crystal structure of its complex with a *C*-terminal domain of sEH was obtained and resolved. These data fully validate **(+)-22** as a new non-racemic advanced lead compound for further development as a potential therapeutic agent for use in such areas as cardiovascular disease, inflammation and pain.

Keywords: Prins reaction; spirocyclic; 1-oxa-9-azaspiro[5.5]undecan-4-amine; orthogonal periphery group variation; oral bioavailability; low LogD; phosphate buffer solubility; eutomer; distomer; protein-ligand crystal structure.

1. Introduction

Epoxy-fatty acids (formed via cytochrome oxidation of polyunsaturated fatty acids) are metabolized primarily via the hydrolytic opening of the epoxide into a vicinal diol (dihydroxy eicosatrienoic acid or DHET) via a catalytic addition of a water molecule (Figure 1).[1,2] In mammals, this fundamental biochemical transformation is catalyzed by the enzyme soluble epoxide hydrolase (sEH, E.C. 3.3.2.10) whose diversity of substrates encompasses epoxyeicosatrienoic acids (EETs), and epoxides of docosahexaenoic acid, referred to as EpDPEs.[3,4] The status of sEH as a biological target for therapeutic intervention is supported by the fact the EETs (i. e. the substrates degraded by the enzyme) carry a plethora of beneficial physiological effects including vasodilation, vasoprotection and antiinflammation.[5-7] Thus, inhibition of sEH represents a potential way of elevating the levels of EETs and thus a promising therapeutic approach to treatment of cardiovascular disease, inflammation and pain.[8-10]

Figure 1. Formation and hydrolytic opening of EETs.
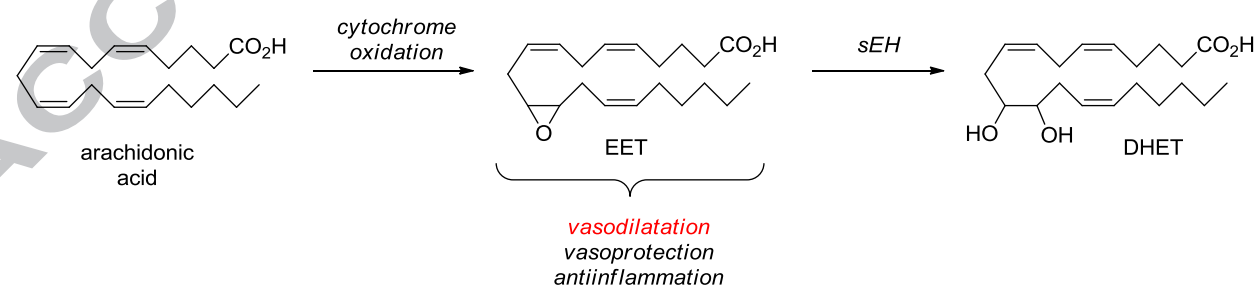
The catalytic site of sEH is very well characterized: the epoxide opening activity of the enzyme is realized via a cooperative action of Tyr381, Tyr465, and Asp333 residues. Urea and amides represent the most popular and potent class of sEH inhibitors and act via mimicking the epoxide binding in the hydrolase site.[11] Interestingly, even very simple, *N,N'*-disubstituted symmetrical ureas represent distinctly potent sEH inhibitors.[12-15] However, symmetrical ureas are generally characterized by lower solubility, which limits their use as *in vivo* pharmacological agents. One

of the common strategies to overcome poor solubility is the introduction of polar groups outside of the main pharmacophore, a strategy which has been applied to sEH inhibitors by Kim et al.[14] However, the evolutionary pathway in the design of urea sEH inhibitors went in the direction of creating non-symmetrical ureas including heterocyclic moieties.[16] Another strategy to increase the solubility is to increase the carbon bond saturation, defined by fraction sp³ (Fsp³), which has correlated with improved solubility, and even with the higher development stage along the drug discovery pipeline.[17] As spirocyclic scaffolds dramatically increase Fsp³, polar spirocyclic scaffolds were successfully employed as the basis for sEH inhibitor design. Particularly relevant as a background to the present study are i. spirocyclic 2,8-diazaspiro[4.5]decane-based trisubstituted urea **1**[18] and ii. 1-oxa-4,9-diazaspiro[5.5]undecane-based trisubstituted urea **2**[19] reported by Toray Industries, whose lowered cLogP values ensure better inhibitor solubility. Recently, we were engaged in the development of preparative approaches to spirocyclic scaffolds related to **2** for the design of free fatty acid receptor 1 agonists.[20] Inspired by the positive example from Toray Industries, we set of to investigate exocyclic amino group containing ureas **3**.

Figure 2. Spirocyclic urea sEH inhbitors: reported previously (**1** and **2**) and investigated in this work (**3**).
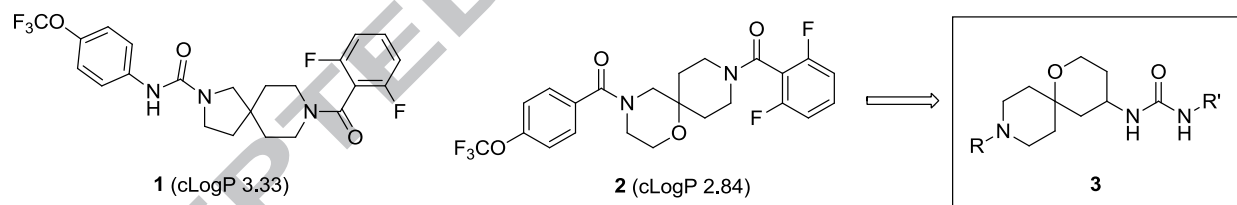
The compounds are distinctly related and represent chiral, disubstituted urea versions of inhibitors **2** (Figure 2). Herein, we report the results of developing ureas **3** as novel, polar, non-racemic type of sEH inhibitors.

2. Results and discussion

Scheme 1. Synthesis of the key spirocyclic building blocks **7** and **9** for sEH inhibitor development.
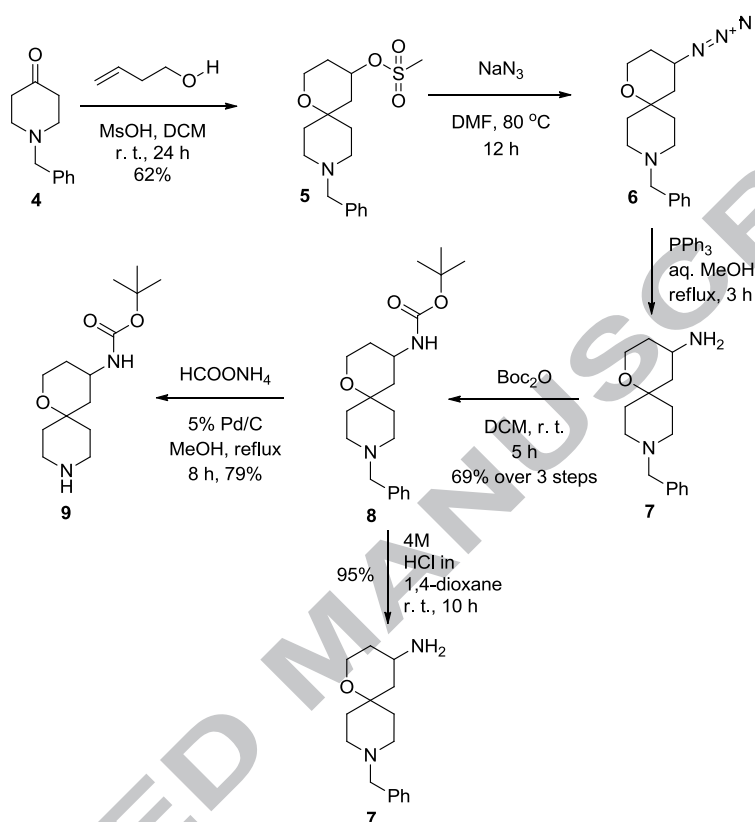

The spirocyclic 9-benzyl-1-oxa-9-azaspiro[5.5]undecan-4-yl methanesulfonate (**5**) was obtained via the Prins reaction of *N*-benzylpiperidone (**4**) with homoallylic alcohol in presence of methanesulfonic acid.[21] The mesylate group in spirocyclic adduct **5** was replaced by azide group and the latter was reduced by the action of triphenylphosphine. Primary spirocyclic amine **7** thus obtained turned out to be difficult to purify chromatographically, impurities co-eluting with **7** regardless of separation conditions employed. Thus, without further purification, **7** was protected with *tert*-butoxycarbonyl (Boc) group and the respective doubly protected spirocyclic bis-amine **8** was obtained in analytically pure form after simple crystallization in a respectable 69% yield over 3 steps (from **5**). The doubly protected building block **8** was envisioned as a precursor to a series of compounds containing independently and orthogonally manipulated molecular periphery around the 1-oxa-9-azaspiro[5.5]undecane core. To this end, the benzyl group in **8** was removed on multigram scale by transfer hydrogenation over 5% Pd/C and analytically pure spirocyclic piperidine **9** was thus available for the initial library development. As a reference set, we envisioned developing a small series of exocyclic urea compounds where the benzyl substituent on the piperidine nitrogen would be kept unchanged (*vide infra*). To this end, primary

amine **7** was re-generated as a free base from purified **8** by removal of the Boc group and neutralization of the respective hydrochloride salt (Scheme 1).

In order to determine what molecular periphery would be optimal for binding of the compounds based on 1-oxa-9-azaspiro[5.5]undecane core (i. e. what groups should be optimally varied on the piperidine *vs.* exocyclic NH_2 nitrogen atoms of key building block **9**), we performed docking of a small set of compounds derived from simple orthogonal modifications of reactive centers of **9**. It was established that for optimal binding, the piperidine nitrogen could be substituted with a small, strongly electron-withdrawing substituent such as acetyl group while the pimary exocyclic group (after the Boc group removal) could be reacted with a benzyl-type isocyanate to produce the pharmacophoric urea fragment. Interestingly, 4-trifluoromethoxybenzyl group in this context appeared to be highly favored, which drew a parallel with compounds from Toray Industries (Figure 2). The optimal substitution pattern established by docking is illustrated by the structure of *N*-mesyl-*N*'-[(4-trifluoromethoxy)benzyl]carbonyl compound (further numbered as compound **11**) docked into the publicly available[22] crystal structure of sEH (PDB code 4OD0, Figure 3).

Figure 3. Docking of a representative compound (**11**) into the crystal structure of sEH.
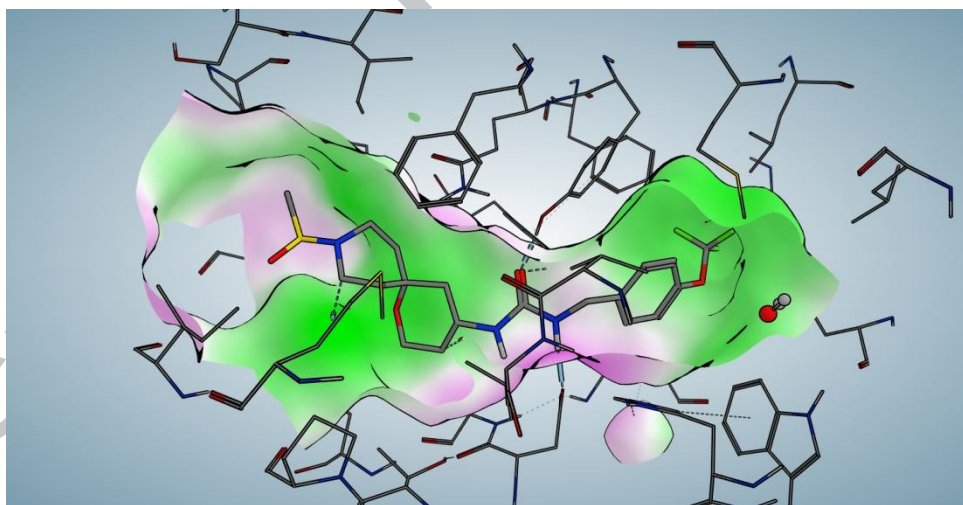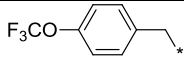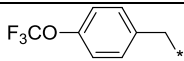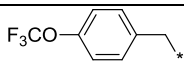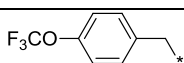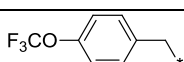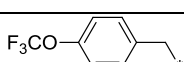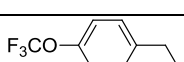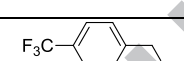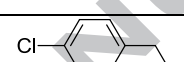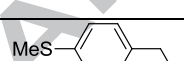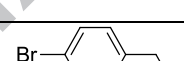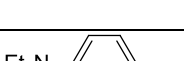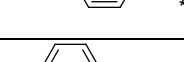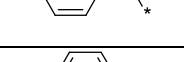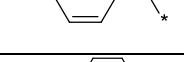
Based on the results of this preliminary *in silico* design of the pilot series of compounds belonging to general formula **3**, we synthesized 22 spirocyclic compounds **11**-**32** in which orthogonal variations of both periphery groups R and R' was explored. First, the piperidine nitrogen in **9** was modified by a sulfonylating (**10**-**11**, **21**-**22**, **25**-**32**), acylating (**12**, **14**-**18**, **24**), alkoxycabonylating (**13**, **19**) or carbamoylating (**20**, **23**) agent. The Boc group from the exocyclic primary amino group was subsequently removed by treatment with 4M HCl in 1,4-dioxane, the solution of the deprotected primary amine neutralized and the target urea was obtained by treatment of the resulting material with an isocyanate at room temperature (Scheme 2).

Scheme 2. Synthesis of spirocyclic sEH inhibitors based on core building block **9**.
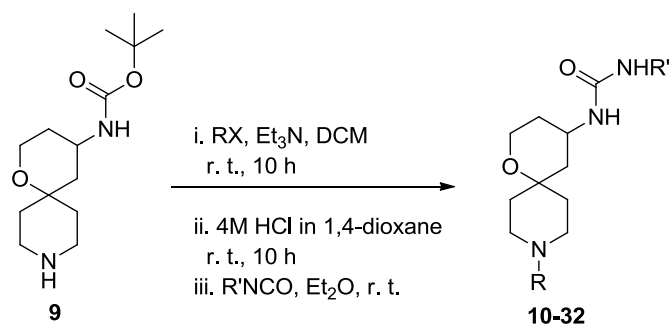
Notably, the majority of ureas were of benzylic type (with a particular emphasis on 4-(trifluoromethoxy)benzyl substitution predicted as the most favorable by *in silico* docking). However, we also included an adamant-1-yl urea as a reference compound since adamantly moieties had earlier found significant prominence as compound periphery elements in the design of sEH inhibitors.[23] Compounds **10**-**32** were tested in a chromogenic substrate sEH inhibition assay and the inhibition data thus obtained revealed a number of SAR generalizations (Table 1).

Table 1. sEH inhibitory activity of spirocyclic compounds **10-32** with variation of both periphery groups.
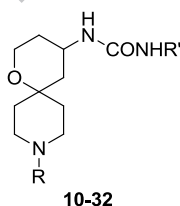
Entry	R	R'	sEH IC$_{50}$ ± SD^{a}(nM)
10	Ms	adamant-1-yl	50.8 ± 1.0
11	Ms	F$_3$CO—⟨benzyl⟩	98.5 ± 3.9
12	Ac	F$_3$CO—⟨benzyl⟩	121 ± 9.0
13	Boc	F$_3$CO—⟨benzyl⟩	5.52 ± 0.43
14	EtCO	F$_3$CO—⟨benzyl⟩	40.3 ± 2.6
15	*i*-PrCO	F$_3$CO—⟨benzyl⟩	41.8 ± 7.9
16	*i*-PrCH$_2$CO	F$_3$CO—⟨benzyl⟩	25.6 ± 3.3
17	*n*-PrCO	F$_3$CO—⟨benzyl⟩	31.4 ± 6.9

ACCEPTED MANUSCRIPT

18	*cyclo*-PrCO	F₃CO—C₆H₄—CH₂—*	36.3 ± 2.9
19	EtOCO	F₃CO—C₆H₄—CH₂—*	16.9 ± 1.1
20	Me₂NCO	F₃CO—C₆H₄—CH₂—*	56.5 ± 4.1
21	EtSO₂	F₃CO—C₆H₄—CH₂—*	26.9 ± 1.1
22	*i*-PrSO₂	F₃CO—C₆H₄—CH₂—*	12.0 ± 1.9
23	*n*-PrNHCO	F₃CO—C₆H₄—CH₂—*	46.8 ± 4.0
24	MeO₂C(CH₂)₂CO	F₃CO—C₆H₄—CH₂—*	53.4 ± 4.3
25	Ms	F₃C—C₆H₄—CH₂—*	41.8 ± 3.6
26	Ms	Cl—C₆H₄—CH₂—*	57.6 ± 0.8
27	Ms	MeS—C₆H₄—CH₂—*	13.2 ± 1.3
28	Ms	Br—C₆H₄—CH₂—*	38.3 ± 1.2
29	Ms	Et₂N—C₆H₄—CH₂—*	62.9 ± 2.1
30	Ms	C₆H₅—CH₂—*	513 ± 54
31	Ms	Me—C₆H₄—CH₂—*	58.0 ± 4.3
32	Me₂NSO₂	F₃CO—C₆H₄—CH₂—*	14.4 ± 0.4

a Mean IC_{50} determined in three independent experiments.

Firstly, the data shown in Table 1 demonstrate the fundamental correctness of the *in silico* predictions for the optimal compound periphery. All 22 compounds **10**-**32** demonstrated full inhibition of sEH and the most potent compounds (**13**, **22**, **27** and **32**) were indeed those 'decorated' with 4-(trifluoromethoxy)benzyl periphery. Limitations of the *in silico* prioritization approach are clearly illustrated by the fact that the compound for which an 'ideal' fit into the sEH active site was predicted by docking (**12**) turned out be rather weak inhibitor (IC_{50} 121 ± 9.0 nM) of the enzyme. Likewise, adamantyl periphery (compound **10**) did not deliver a lead potency level in this series. In general, the SAR is very pronounced in this series and the compounds′ potency appears to be very sensitive to the small variations in the periphery

substituents. In order to appreciate this, it suffices to note the drop in inhibitory activity observed, for instance, on 'removing' 4-methylthio substituent in **27** (IC$_{50}$ 13.2 ± 1.3 nM): the respective unsubstituted compound **30** displayed ~50 times lower potency (IC$_{50}$ 513 ± 54 nM). Likewise, 'replacement' of the Boc group in the most potent compound (**13**, IC$_{50}$ 5.52 ± 0.43 nM) with an acetyl group led to >50-fold drop in potency (compound **12**, IC$_{50}$ 121 ± 9.0 nM).

The SAR reference set of 13 compounds (**33**-**45**) where the substituent on the piperidine nitrogen was kept unchanged (Bn) was synthesized in a very simple fashion by treatment of primary amine **7** with a range of aromatic and aliphatic isocyanates (Scheme 3). In all cases, the respective ureas, when formed, precipitated from the ethereal solution, which significantly facilitate their isolation in analytically pure form (simple filtration).

Scheme 3. Synthesis of spirocyclic sEH inhibitors based on core building block **7**.
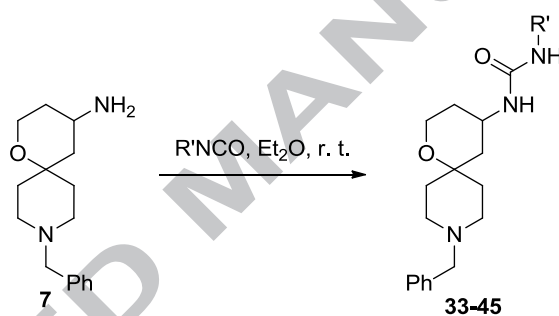
As it had been, in principle, also predicted by *in silico* docking experiments, the benzyl group on the piperidine nitrogen did not permit optimal binding at the sEH active site (as opposed to small electron-withdrawing groups displayed in the compounds shown in Table 1). Therefore, all compounds **33**-**45** (Table 2) turned out to be either weak inhibitors of sEH (**33**-**43**) or even completely inactive (**44**-**45**). Even the activity of the most potent compound in this series (**37**, IC$_{50}$ 93.8 ± 8.2 nM) is dwarfed by the low nanomolar activity of some of the compounds from the series described in Table 1 (e. g., compounds **13**, **22**, **27** and **32**). This clearly demonstrates the requirement for a structurally simple, strongly electron-withdrawing substituent to be present on the piperidine nitrogen of 1-oxa-9-azaspiro[5.5]undecan-4-amine-derived ureas in order to exhibit high inhibitory potency against sEH.

Table 2. sEH inhibitory activity of spirocyclic compounds **33**-**45** substituted with benzyl group at the piperidine nitrogen atom.

33-45
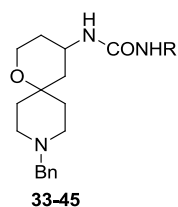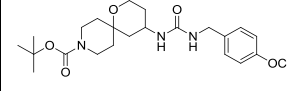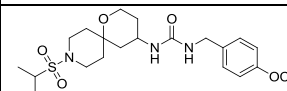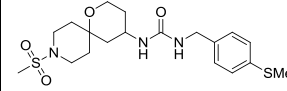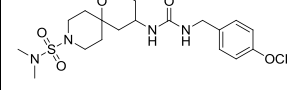
Entry	R	sEH IC$_{50}$ ± SD^a (nM)
33		112 ± 12.6
34		2,090 ± 150
35		194 ± 12.0
36		115 ± 10.0
37		93.8 ± 8.2
38		161 ± 6.0
39		250 ± 31.0
40		210 ± 39.0
41		285 ± 6.0
42		628 ± 24.0
43	adamant-1-yl	428 ± 10.0
44		>10,000
45		>10,000

^{a} Mean IC$_{50}$ determined in three independent experiments.

It should be noted that the initial profiling of compounds **10**-**45** as sEH inhibitors was performed for racemic mixtures. The next step in the development of a novel sEH inhibitor based on the spirocyclic chemotype idea described herein was to nominate the lead racemic compound, obtain the compound in the form of pure enantiomers, establish their absolute configuration, establish which enantiomer acts as a eutomer (while the other being distomer) and confirm the relevant binding mode of the eutomer to the enzyme by crystallographic experiments.

With an upper potency cutoff of 15 nM, compounds **13**, **22**, **27** and **32** were considered as candidates for racemic lead compound nomination (Table 3). Notably, all four compounds displayed remarkably high solubility in phosphate buffer solution. Likewise, the compounds were established as unusually polar entities for the sEH inhibitor realm, confirming the assumption that a high-F_{sp3} scaffold would enhance solubility. Indeed, their experimentally measured $logD_{7.4}$ values were in the range 0.69 – 1.19 and correlated in general rather well with the calculated values. The high polarity of these compounds clearly makes them distinct not only from the related spirocyclic ureas **1** and **2** (*vide supra*) but, particularly, from the earlier reported adamantyl-substituted low nanomolar inhibitors of sEH[24] (somewhat akin to compound **10**) which are significantly more lipophilic. Certainly, potency level alone could not be considered as a single criterion for lead compound nomination as potential metabolic and permeability issues should be taken into account. For instance, the most potent racemic compound in the series (**13**, IC_{50} 5.52 ± 0.43 nM) was not considered a potential lead compound based on known tendency of the Boc group to undergo hydrolytic cleavage *in vivo* (thus presenting a metabolic liability). Oxidizable character of divalent sulfur gave a similar reason for excluding compound **23** from consideration as a lead racemic compound. Thus, the choice essentially was reduced to selecting between isosteric compounds **22** and **32** having very similar inhibitory activity (IC_{50} 12.0 ± 1.9 and 14.4 ± 0.4 nM, respectively). The final nomination of **22** as the lead racemic compound was to a certain degree rather obvious because **32** contains one extra sulfonamide bond which can be expected to significantly lower intestinal absorption and cellular permeability of **32** compared to **22**.[25]

Table 3. Nomination of a racemic lead sEH inhibitor among compounds **13**, **22**, **27** and **32**.

Entry	Structure	sEH IC_{50} ± SD (nM)	PB solubility $(mM)^a$	$LogD_{7.4}$ HPLC	LogD MOE software $(pH\ 7)^b$	Comments
13		5.52 ± 0.43	>0.5	1.19	2.51	Potency leader. Carbamate moiety is prone to hydrolysis and may present a metabolic liability.
22		12.0 ± 1.9	>0.5	0.99	1.33	Nominated as the lead racemic inhibitor.
23		13.2 ± 1.3	>0.5	0.69	0.45	Oxidizable divalent sulfur substituent.
32		14.4 ± 0.4	>0.5	1.04	1.08	One extra sulfonamide bond affecting absorption properties.

[a] Measured by absorption of phosphate buffer (PB) solutions containing 0.01% Tween and 1% DMSO.

[b] Calculated using Molecular Operating Environment software by Chemical Computing Group (https://www.chemcomp.com/MOE-Molecular_Operating_Environment.htm).
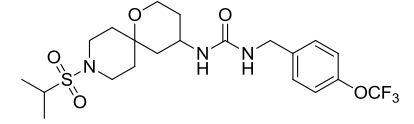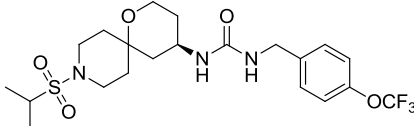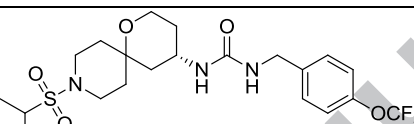
Having nominated compound (±)-22 as the lead racemic compound, we were keen to establish its pharmacokinetic profile. The pharmacokinetic characterization of (±)-22 was performed in male JAXC57BL/6J mice (see Experimental Section) on oral as well as intravenous administration of 10 mg/kg of the drug. The compound generally demonstrated excellent absorption and elimination characteristics as well as remarkable (46.3%) absolute oral bioavailability (Table 4). This encouraged us to invest further effort in the development of compound 22 in non-racemic form.

Table 4. Pharmacokinetic parameters of compound (±)-22.

Pharmacokinetic parameters	IV Bolus Administration (10 mg/kg)	PO Extravascular Administration (10 mg/kg)
T_{max} (min)	10	10
C_{max} (ng/mL)	3931	1507
C_0 (ng/mL)	5900 (extrapolated)	0 (set to 0)
Lambda (z) (min)	0.0219	0.0168
HL Lambda (min)	31.6	41.3
AUC_{last} (min x ng/mL)	183700	83630
AUC_{Inf} obs (min x ng/mL)	18400	85480
AUC_{Extrap} obs (%)	0.49	2.17
V_z obs (mL/kg)	2470	-
Cl obs (mL/min/kg)	54.2	-
V_{ss} obs (mL/kg)	1700	-
F (%)	-	46.3

The racemic (±)-22 was separated into individual enantiomers identified as (+)-22 and (-)-22 using theoretical calculations as well as circular dichroism spectra (see Experimental Section). Individual testing (Table 5) of (+)-22 and (-)-22 against sEH demonstrated that the inhibitory activity initially observed for the racemate (IC_{50} 10.8 ± 0.74 nM) primarily resides with the dextrorotatory eutomer (+)-22 (IC_{50} 4.99 ± 0.18 nM) while the distomer (-)-22 is >10 times less active (IC_{50} 54.8 ± 4.93 nM). Clearly, non-racemic compound (+)-22 represents a promising lead compound for the development of novel pharmaceutical agent acting as an efficient inhibitor of soluble epoxide activity.

Table 5. Comparison of sEH inhibitory activity of racemic inhibitor **22** with that of (+)- and (-)-enantiomers.

Compound	Structure	sEH IC$_{50}$ ± SD (nM)
(±)-**22**		10.8 ± 0.74
(+)-**22**		4.99 ± 0.18
(-)-**22**		54.8 ± 4.93

In order to confirm the relevance of the inhibitor's binding mode to the inhibition of the catalytic activity, we cloned, expressed and purified *C*-terminal domain of sEH and soaked the crystals of this protein construct with a solution of **(+)-22** in DMSO/PEG 400 (see Experimental Section). The crystal structure of the inhibitor co-crystallized with *C*-terminal domain of the target was resolved and demonstrated that the binding of **(+)-22** indeed took place at the enzyme's active site and the affinity of the former to the latter was supported by a network of hydrogen bonds towards Asp335, Tyr383, and Tyr336 as well as hydrophobic and π-stacking interaction. Most notably, both rings of the spirocyclic core accommodate the favorable boat-like conformation and fit complementary into the hydrophobic tunnel of sEH, which would explain the potency difference between the both enantiomers of (±)-**22**. The structure of the protein-ligand complex was solved at 2.26Å resolution. In the initial mFo-DFc electron density map obtained after molecular replacement with the model without a ligand, the pronounced bulky positive electron density was identified in the vicinity of active site of sEH enzyme. The properties of the obtained 2mFo-DFc map allowed unambiguous placement of (+)-**22** in the unique orientation in the active site of sEH enzyme. The correctness of the ligand placement in the final model was further corroborated by the polder omit map (Figure 4A). The superposition of the X-ray structure of **(+)-22** with the proposed binding mode of **11** reveals the error in binding mode proposed by molecular docking, which is caused by the water molecule Wat702 (Figure 4B). The trifluoromethyoxy group of **(+)-22** displaces Wat702, thereby allowing the benzyl moiety to accommodate a different conformation in the lipophilic pocket.
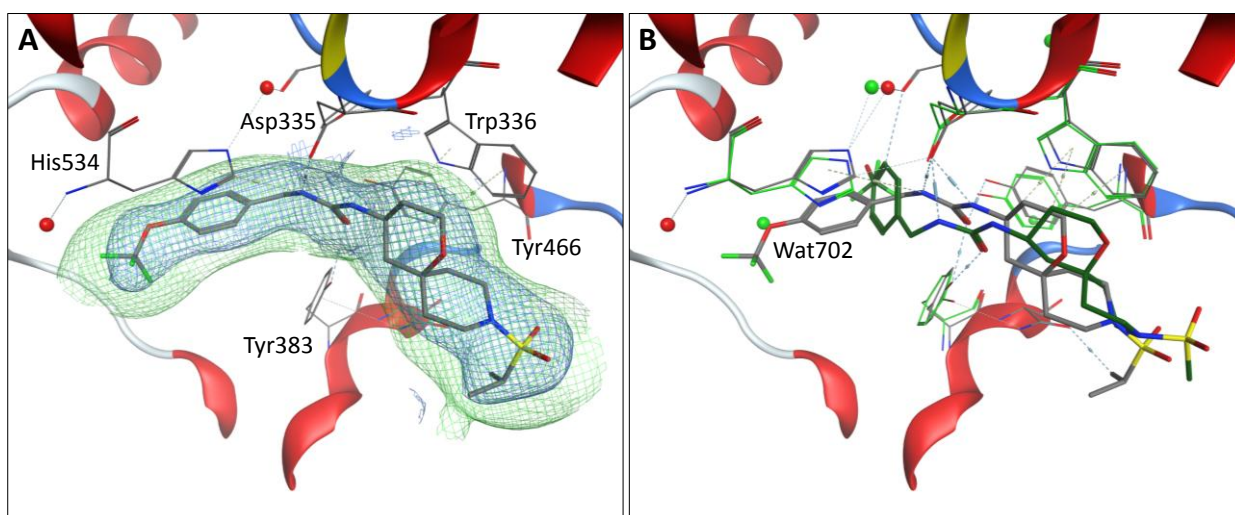
Figure 4. (A) Ligand interactions in the X-ray crystallographic structure of C-terminal domain of sEH in complex with **(+)-22**. The positive 2mFo-DFc difference map (blue mesh contoured at 1σ) and mFo-DFc polder omit map (green mesh) with solvent exclusion radius of 3Å and contoured at 3σ around **(+)-22** ligand were calculated from the final model of the protein-ligand complex (PDB: 6FR2). Ligand and neighboring protein environment are shown as stick models. The dashed lines indicate the interactions of **(+)-22** with key residues of the active site. (B) Superposition of the binding mode of **11** proposed by molecular docking with the **(+)-22** (RMSD = 0.305Å). Green sticks indicate **11**, green lines - the enzyme, green spheres - the water molecules (PDB: 4OD0).

3. Conclusions

Based on the Prins chemistry-derived spirocyclic template, we designed and synthesized an SAR-probing library and tested it against sEH. Four most potent racemic inhibitors (IC$_{50}$ < 15 nM) were considered as potential lead compounds based on the potency as well as remarkably good solubility in phosphate buffer solution and low values of experimentally determined logD values. One such racemic compound (**22**) showed excellent oral bioavailability and other pharmacokinetic characteristics in mice. Crystal structure of the complex of extrorotatory eutomer **(+)-22** (IC$_{50}$ 4.99 ± 0.18 nM) with the *C*-terminal domain of sEH was obtained and resolved to reveal an efficient binding of the inhibitor in the active site of the enzyme. In summary, we have developed and reported the synthesis and characterization of a new polar, highly soluble, orally bioavailable, non-racemic, spirocyclic inhibitor of soluble epoxide hydrolase **(+)-22**.

4. Experimental section

4.1. General experimental

All reactions were conducted in oven-dried glassware in atmosphere of nitrogen. Melting points were measured with a Buchi B-520 melting point apparatus and were not corrected. Analytical thin-layer chromatography was carried out on Silufol UV-254 silica gel plates using appropriate mixtures of ethyl acetate and hexane. Compounds were visualized with short-wavelength UV light. ^{1}H NMR and ^{13}C NMR spectra were recorded on Bruker MSL-300 and 400 MHz spectrometers in DMSO-d_6 or CDCl$_3$ using TMS as an internal standard. Mass spectra were recorded using Shimadzu LCMS-2020 system with electron-spray (ESI) ionization. All reagents and solvents were obtained from commercial sources and used without further purification. Elemental analyses were obtained at Research Institute for Chemical Crop Protection (Moscow, Russia) using Carlo Erba Strumentazione 1106 analyzer. Optical rotation was measured on a Bellingham Stanley Ltd. ADP440/ADP440+ model digital polarimeter at 589 nm wavelength.

4.2 Synthetic organic chemistry

4.2.1. Starting materials

9-Benzyl-1-oxa-9-azaspiro[5.5]undecan-4-yl methanesulfonate (**5**) was synthesized in 5-10 g portions as described previously.[21]

4.2.2. *tert*-Butyl (9-benzyl-1-oxa-9-azaspiro[5.5]undec-4-yl)carbamate (8)

9-Benzyl-1-oxa-9-azaspiro[5.5]undecan-4-yl methanesulfonate (**5**, 20 g, 58.92 mmol) was dissolved in anhydrous DMF (100 mL). Sodium azide (9.575 g, 147.3 mmol) was added in portions with stirring. The stirring continued for 12 h while the reaction mixture was heated at 80 °C on an oil bath. The mixture was cooled to ambient temperature, poured into water (200 mL) and the resulting turbid mixture was extracted with ethyl acetate (2x100 mL). The combined organic extracts were washed with sat. aq. NaHCO$_3$ solution, dried over anhydrous Na$_2$SO$_4$, filtered and concentrated *in vacuo*. The residue was dissolved in methanol (100 mL) and water (3.0 mL) was added. Triphenylphosphine (23.181 g, 88.38 mmol) was added in small portions and the resulting mixture was heated at reflux for 3 h. The volatiles were removed on a rotatory evaporator, the residue was dissolved in CH$_2$Cl$_2$ (100 mL) and the solution was extracted with 30% aqueous citric acid. The acidic aqueous extract was neutralized with K$_2$CO$_3$ and extracted with CH$_2$Cl$_2$ (2 x 100 mL). The combined organic extracts were dried over anhydrous Na$_2$SO$_4$, filtered and concentrated *in vacuo*. The residue was triturated with 7:3 hexane-diethyl ether mixture and the crystalline residue thus formed was separated by filtration and washed with

diethyl ether. The solid residue was dried *in vacuo*. Then it was dissolved in CH_2Cl_2 (100 mL) and treated with di-*tert*-butyl carbonate (8.883 g, 50.98 mmol) added in small portions. The resulting mixture was stirred at ambient temperature for 5 hours and concentrated *in vacuo*. The residue was crystallized from 1:1 mixture of hexane-diethyl ether. The crystalline product was separated by filtration, washed with hexane and dried in high vacuum to give the title compound as a white crystalline solid (m.p. 134-136 ºC). Yield 14.5 g (69%). ^{1}H NMR (300 MHz, CDCl$_3$) δ 7.36 – 7.21 (m, 5H), 4.46 – 4.24 (m, 1H), 3.85 – 3.70 (m, 2H), 3.68 – 3.55 (m, 1H), 3.53 (s, 2H), 2.67 – 2.51 (m, 2H), 2.50 – 2.35 (m, 1H), 2.35 – 2.22 (m, 1H), 2.11 (d, *J* = 13.7 Hz, 1H), 1.97 – 1.80 (m, 2H), 1.74 – 1.50 (m, 3H), 1.45 (s, 9H), 1.39 – 1.24 (m, 1H), 1.13 (t, *J* = 12.4 Hz, 1H). ^{13}C NMR (75 MHz, DMSO-*d*$_6$) δ 155.1, 138.1, 129.2, 128.2, 127.1, 79.4, 71.1, 63.1, 59.5, 48.9, 48.7, 43.7, 42.9, 39.1, 33.7, 29.4, 28.4. Anal. Calcd for $C_{21}H_{32}N_2O_3$: C, 69.97; H, 8.95; N, 7.77; found C, 70.02; H, 8.91; N, 7.81.

4.2.3. *tert*-Butyl (1-oxa-9-azaspiro[5.5]undec-4-yl)carbamate (9)

tert-Butyl (9-benzyl-1-oxa-9-azaspiro[5.5]undec-4-yl)carbamate (**8**, 8.5 g, 24 mmol) was dissolved in methanol (100 mL). Ammonium formate (6.06 g, 96 mmol) was added in protions followed by 5% Pd/C (0.43 g). The reaction mixture was heated at reflux for 8 h, cooled down to room temperature, filtered through a pad of celite. The filtrate was concentrated in vacuo and the residue was extracted with CH_2Cl_2 (3 x 50 mL). The combined organic extracts were washed with brine, dried over anhydrous Na_2SO_4, filtered and concentrated in vacuo to give the title compound as clear oil. Yield – 5.1 g (79.2%). ^{1}H NMR (300 MHz, CDCl$_3$) δ 6.75 (d, *J* = 7.6 Hz, 1H), 3.65 – 3.47 (m, 4H), 3.01 – 2.55 (m, 3H), 2.02 – 1.85 (m, 1H), 1.71 – 1.55 (m, 2H), 1.43 – 1.24 (m, 14H), 1.07 (t, *J* = 12.1 Hz, 1H). ^{13}C NMR (75 MHz, DMSO-*d*$_6$) δ 154.8, 79.2, 77.5, 71.1, 58.8, 42.8, 42.2, 41.3, 32.8, 30.3, 28.3. Anal. Calcd. For $C_{14}H_{26}N_2O_3$: C, 62.19; H, 9.69; N, 10.36; found C, 62.22; H, 9.71; N, 10.33.

4.2.4. 9-Benzyl-1-oxa-9-azaspiro[5.5]undecan-4-amine (7)

tert-Butyl (9-benzyl-1-oxa-9-azaspiro[5.5]undec-4-yl)carbamate (**8**, 4.0 g, 11.09 mmol) was dissolved in 4M HCl in 1,4-dioxane (8.3 mL, 33.27 mmol) and the resulting mixture was stirred for 10 h. The reaction mixture was concentrated in vacuo and the residue was neutralized with sat. aq. K_2CO_3 to give the title compound as clear oil. Yield – 2.83 g (94.6%). ^{1}H NMR (300 MHz, CDCl$_3$) δ 11.24 – 11.02 (m, 1H), 8.30 – 8.14 (m, 3H), 7.71 – 7.59 (m, 2H), 7.50 – 7.39 (m, 3H), 4.27 (d, *J* = 4.6 Hz, 2H), 3.73 (dd, *J* = 12.0, 4.6 Hz, 1H), 3.60 – 3.45 (m, 1H), 3.16 – 3.00 (m, 3H), 2.93 – 2.75 (m, 1H), 2.49 – 2.40 (m, 1H), 2.22 – 1.31 (m, 8H). ^{13}C NMR (75 MHz, CDCl$_3$) δ 131.4, 129.8, 129.3, 128.6, 68.4, 58.6, 46.7, 43.3, 35.0, 29.8, 25.5. Anal. Calcd. for $C_{16}H_{24}N_2O$: C, 73.81; H, 9.29; N, 10.76; found C, 73.86; H, 9.33; N, 10.72.

4.2.5. General procedure for preparation of compounds 10-32.

Tert-Butyl (1-oxa-9-azaspiro[5.5]undec-4-yl)carbamate (**9**, 2 g, 74 mmol) was dissolved in CH_2Cl_2 (15 mL) and triethylamine (1.2 mL, 89 mmol) was added dropwise. Within 30 min, the respective acylating, sulfonylating or carbamoylating agent (81 mmol) was added dropwise. The resulting mixture was stirred at ambient temperature for 10 h, washed with 5% aqueous citric acid, 10% aqueous K_2CO_3 and the organic phase was dried over anhydrous Na_2SO_4, filtered and concentrated *in vacuo*. The residue was dissolved in 4M HCl in 1,4-dioxane (2.65 mL) and stirred at ambient temperature for 10 h. The volatiles were removed *in vacuo* and the residue was neutralized with saturated aqueous K_2CO_3 to provide clear oil. The requisite portion of the primary amine (0.58 mmol) thus obtained was dissolved in 1,4-dioxane (10 mL) and treated with the respective isocyanate (0.61 mmol). The reaction mixture was stirred overnight, poured into water (25 mL) and extracted with ethyl acetate (2 x 25 mL). The combined organic phase was washed with 3% aqueous citric acid, dried over anhydrous Na_2SO_4, filtered and concentrated *in vacuo*. The residue was purified by column chromatography on silica gel using 0→2% MeOH in CH_2Cl_2 as eluent. The fractions containing the product were combined, concentrated *in vacuo* to provide the title compound.

4.2.5.1. *N*-1-Adamantyl-*N′*-[9-(methylsulfonyl)-1-oxa-9-azaspiro[5.5]undec-4-yl]urea (10)

Yield – 37 mg (15.1%). White solid, m.p. 121-124 ºC. ^{1}H NMR (300 MHz, DMSO-*d6*) δ 5.54 (d, *J* = 7.6 Hz, 1H), 5.40 (s, 1H), 3.69 – 3.61 (m, 2H), 3.56 – 3.47 (m, 1H), 3.29 – 3.21 (m, 2H), 3.02 – 2.91 (m, 1H), 2.84 (s, 3H), 2.83 – 2.74 (m, 1H), 2.23 (br d, *J* = 14.0 Hz, 1H), 1.99 (br s, 3H), 1.84 (br s, 6H), 1.76 – 1.67 (m, 2H), 1.64 – 1.53 (m, 8H), 1.47 – 1.33 (m, 1H), 1.27 – 1.08 (m, 1H), 1.01 (t, *J* = 12.4 Hz, 1H); ^{13}C NMR (75 MHz, DMSO-*d6*) δ 156.7, 70.1, 59.5, 49.7, 42.9, 42.2, 41.7, 41.5, 41.4, 41.1, 38.1, 36.3, 34.0, 33.7, 29.2, 28.7; HRMS (ESI) *m/z* calcd for $C_{21}H_{36}N_3O_4S$ [M+H^{+}] 482.0719, found 482.0725.

4.2.5.2. *N*-[9-(Methylsulfonyl)-1-oxa-9-azaspiro[5.5]undec-4-yl]-*N′*-[4-(trifluoromethoxy)-benzyl]urea (11)

Yield – 42 mg (15.5%). M. p. 96-98 ºC. ^{1}H NMR (300 MHz, DMSO-*d6*) δ 7.39 – 7.25 (m, 4H), 6.31 (t, *J* = 5.8 Hz, 1H), 5.91 (d, *J* = 7.8 Hz, 1H), 4.21 (d, *J* = 5.8 Hz, 2H), 3.82 – 3.62 (m, 2H), 3.60 – 3.48 (m, 1H), 3.29 – 3.22 (m, 2H), 3.04 – 2.91 (m, 1H), 2.84 (s, 3H), 2.82 – 2.74 (m, 1H), 2.31 – 2.18 (m, 1H), 1.80 – 1.69 (m, 2H), 1.67 – 1.50 (m, 2H), 1.48 – 1.34 (m, 1H), 1.31 – 1.17 (m, 1H), 1.16 – 1.05 (m, 1H). ^{13}C NMR (75 MHz, DMSO-*d6*) δ 157.4, 147.1 (q, *J* = 1.7 Hz), 140.7, 128.9, 120.2 (d, *J* = 255.7 Hz), 121.0, 69.9, 59.3, 42.6, 42.2, 42.1, 41.3, 41.2, 38.0, 33.8, 33.6, 28.6. HRMS (ESI) *m/z* calcd for $C_{19}H_{27}F_3N_3O_5S$ [M+H^{+}] 466.1540, found 466.1586.

4.2.5.3. 1-(9-Acetyl-1-oxa-9-azaspiro[5.5]undec-4-yl)-3-(4-trifluoromethoxybenzyl)urea (12)

Yield – 196 mg (78,7%), clear oil. ^{1}H NMR (300 MHz, CDCl$_3$) δ 7.32 – 7.23 (m, 2H), 7.16 – 7.09 (m, 2H), 4.32 (s, 2H), 4.23 – 4.06 (m, 1H), 4.02 – 3.87 (m, 1H), 3.82 – 3.70 (m, 1H), 3.66 – 3.39 (m, 2H), 3.34 – 2.75 (3m, 2H), 2.20 – 2.11 (m, 1H), 2.04 (s, 3H), 1.95 – 1.73 (m, 2H), 1.61 – 1.08 (m, 5H); ^{13}C NMR (75 MHz, DMSO-d_6) δ 168.0, 157.3, 146.9 (d, J = 1.6 Hz), 140.6, 128.7, 120.9, 120.1 (q, J = 255.6 Hz), 70.8, 59.3, 59.2, 42.6, 42.5, 42.1, 41.5, 41.4, 38.2, 36.6, 36.4, 33.5, 29.5, 28.9, 21.3; HRMS (ESI) m/z calcd for C$_{20}$H$_{27}$F$_3$N$_3$O$_4$ [M+H$^+$] 430.1875, found 430.1942.

4.2.5.4. 4-[3-(4-Trifluoromethoxy-benzyl)-ureido]-1-oxa-9-aza-spiro[5.5]undecane-9-carboxylic acid *tert*-butyl ester (13)

Yield 160 mg (70%), clear oil. ^{1}H NMR (300 MHz, CDCl$_3$) δ 7.34 – 7.25 (m, 2H), 7.20 – 7.14 (m, 2H), 4.34 (s, 2H), 4.08 – 3.88 (m, 1H), 3.84 – 3.52 (m, 4H), 3.27 – 3.11 (m, 1H), 3.09 – 2.92 (m, 1H), 2.17 – 2.02 (m, 1H), 1.98 – 1.75 (m, 2H), 1.50 – 1.07 (m, 5H), 1.44 (s, 9H); ^{13}C NMR (75 MHz, DMSO-d_6) δ 157.3, 154.0, 147.0 (q, J = 1.7 Hz), 140.7, 128.8, 120.9, 120.1 (q, J = 255.6 Hz), 78.5, 70.6, 59.2, 42.6, 42.1, 38.3, 33.5, 29.0, 28.1; HRMS (ESI) m/z calcd for C$_{23}$H$_{33}$F$_3$N$_3$O$_5$ [M+H$^+$] 488.2294, found 488.2367.

4.2.5.5. *N*-(9-Propionyl-1-oxa-9-azaspiro[5.5]undec-4-yl)-*N′*-[4-(trifluoromethoxy)benzyl]-urea (14)

Yield – 271 mg (96%). White crystalline solid, m.p. 144-146 ℃. ^{1}H NMR (300 MHz, DMSO-d_6) δ 7.40 – 7.24 (m, 4H), 6.30 (t, J = 6.0 Hz, 1H), 5.89 (d, J = 7.6 Hz, 1H), 4.21 (d, J = 6.0 Hz, 2H), 4.05 – 3.92 (m, 1H), 3.83 – 3.63 (m, 2H), 3.62 – 3.47 (m, 2H), 3.18 – 2.70 (3m, 2H), 2.35 – 2.23 (m, 2H), 2.16 – 2.02 (m, 1H), 1.80 – 1.66 (m, 2H), 1.54 – 1.02 (m, 5H), 0.97 (t, J = 7.6 Hz, 3H). ^{13}C NMR (75 MHz, DMSO-d_6) δ 171.2, 157.4, 147.1 (d, J = 1.7 Hz), 140.7, 128.8, 121.0, 120.2 (q, J = 255.7 Hz), 70.9, 59.4, 59.3, 42.7, 42.6, 42.2, 40.6, 40.5, 39.1, 38.4, 36.9, 36.7, 33.6, 29.7, 29.0, 25.7, 25.6, 9.6. HRMS (ESI) m/z calcd for C$_{21}$H$_{29}$F$_3$N$_3$O$_4$ [M+H$^+$] 444.2032, found 444.2117.

4.2.5.6. *N*-(9-Isobutyryl-1-oxa-9-azaspiro[5.5]undec-4-yl)-*N′*-[4-(trifluoromethoxy)benzyl]-urea (15)

Yield – 246 mg (93%), clear oil. ^{1}H NMR (300 MHz, DMSO-d_6) δ 7.40 – 7.24 (m, 4H), 6.36 (t, J = 6.0 Hz, 1H), 5.93 (d, J = 7.8 Hz, 1H), 4.20 (d, J = 6.0 Hz, 2H), 4.05 – 3.93 (m, 1H), 3.82 – 3.49 (m, 4H), 3.22 – 2.70 (2m, 3H), 2.19 – 2.02 (m, 1H), 1.80 – 1.66 (m, 2H), 1.54 – 1.06 (m, 5H), 0.97 (br d, J = 6.0 Hz, 6H); ^{13}C NMR (75 MHz, DMSO-d_6) δ 174.1, 157.4, 147.0 (q, J = 1.6

Hz), 140.7, 128.8, 120.9, 120.1 (q, J = 255.7 Hz), 71.0, 59.4, 59.3, 42.7, 42.5, 42.1, 40.6, 40.5, 39.4, 38.4, 36.9, 36.8, 33.6, 29.0, 19.5, 19.4; HRMS (ESI) m/z calcd for $C_{22}H_{31}F_3N_3O_4$ [M+H$^+$] 458.2188, found 458.2289.

4.2.5.7. N-[9-(3-Methylbutanoyl)-1-oxa-9-azaspiro[5.5]undec-4-yl]-N'-[4-(trifluoro-methoxy)benzyl]urea (16)

Yield 246 mg (90.1%), clear oil. ^{1}H NMR (300 MHz, DMSO-d_6) δ 7.40 – 7.25 (m, 4H), 6.34 (br t, J = 6.0 Hz, 1H), 5.93 (br d, J = 7.3 Hz, 1H), 4.21 (d, J = 6.0 Hz, 2H), 4.05 – 3.93 (m, 1H), 3.82 – 3.63 (m, 2H), 3.61 – 3.49 (m, 2H), 3.25 – 2.71 (3m, 2H), 2.21 – 2.02 (m, 3H), 2.01 – 1.87 (m, 1H), 1.79 – 1.66 (m, 2H), 1.52 – 1.01 (m, 5H), 0.88 (d, J = 6.5 Hz, 6H); ^{13}C NMR (75 MHz, DMSO-d_6) δ 169.8, 157.3, 147.0 (q, J = 1.8 Hz), 140.7, 128.8, 120.9, 120.1 (q, J = 255.7 Hz), 70.9, 59.4, 59.3, 43.8, 42.7, 42.5, 42.1, 41.2, 41.0, 40.9, 38.4, 36.8, 36.6, 33.6, 33.5, 29.9, 29.1, 25.2, 22.6, 22.5; HRMS (ESI) m/z calcd for $C_{23}H_{33}F_3N_3O_4$ [M+H$^+$] 472.2188, found 472.2412.

4.2.5.8. N-(9-Butyryl-1-oxa-9-azaspiro[5.5]undec-4-yl)-N'-[4-(trifluoromethoxy)benzyl]urea (17)

Yield – 197 mg (74.4%), clear oil. ^{1}H NMR (300 MHz, DMSO-d_6) δ 7.38 – 7.25 (m, 4H), 6.30 (t, J = 6.0 Hz, 1H), 5.88 (d, J = 7.0 Hz, 1H), 4.21 (d, J = 6.0 Hz, 2H), 4.05 – 3.91 (m, 1H), 3.83 – 3.63 (m, 2H), 3.62 – 3.48 (m, 2H), 3.19 – 2.70 (3m, 2H), 2.31 – 2.20 (m, 2H), 2.16 – 2.02 (m, 1H), 1.80 – 1.66 (m, 2H), 1.57 – 1.15 (m, 6H), 1.14 – 1.02 (m, 1H), 0.87 (t, J = 7.0 Hz, 3H); ^{13}C NMR (75 MHz, DMSO-d_6) δ 171.8, 158.9, 148.6 (d, J = 1.6 Hz), 121.9 (q, J = 255.6 Hz), 142.2, 130.4, 122.5, 121.5 (q, J = 256.0 Hz), 72.5, 60.9, 60.8, 44.2, 44.1, 43.7, 42.3, 42.2, 39.9, 38.3, 38.2, 35.9, 35.1, 31.4, 30.6, 19.9, 15.4; HRMS (ESI) m/z calcd for $C_{22}H_{31}F_3N_3O_4$ [M+H$^+$] 458.2188, found 458.2261.

4.2.5.9. N-[9-(Cyclopropylcarbonyl)-1-oxa-9-azaspiro[5.5]undec-4-yl]-N'-[4-(trifluoro-methoxy)benzyl]urea (18)

Yield 241 mg (91.3%), clear oil. ^{1}H NMR (300 MHz, DMSO-d_6) δ 7.41 – 7.24 (m, 4H), 6.37 (t, J = 6.0 Hz, 1H), 5.88 (d, J = 7.8 Hz, 1H), 4.21 (d, J = 6.0 Hz, 2H), 4.03 – 3.84 (m, 2H), 3.83 – 3.64 (m, 2H), 3.63 – 3.50 (m, 1H), 3.09 – 2.70 (2m, 2H), 2.21 – 2.02 (m, 1H), 2.01 – 1.88 (m, 1H), 1.81 – 1.68 (m, 2H), 1.60 – 1.02 (m, 5H), 0.76 – 0.60 (m, 4H); ^{13}C NMR (75 MHz, DMSO-d_6) δ 170.7, 157.4, 147.0 (d, J = 1.5 Hz), 140.7, 128.8, 120.9, 120.1 (q, J = 255.7 Hz), 71.0, 59.3, 42.6, 42.1, 40.7, 38.3, 37.5, 37.3, 33.6, 10.3, 6.8; HRMS (ESI) m/z calcd for $C_{22}H_{29}F_3N_3O_4$ [M+H$^+$] 456.2032, found 456.2094.

4.2.5.10. Ethyl 4-[({[4-(trifluoromethoxy)benzyl]amino}carbonyl)amino]-1-oxa-9-azaspiro[5.5]undecane-9-carboxylate (19)

Yield 246 mg (92.5%), clear oil. ^{1}H NMR (300 MHz, DMSO-d_6) δ 7.39 – 7.25 (m, 4H), 6.30 (t, J = 6.0 Hz, 1H), 5.88 (d, J = 7.8 Hz, 1H), 4.21 (d, J = 6.0 Hz, 2H), 4.01 (q, J = 7.1 Hz, 2H), 3.82 – 3.48 (m, 5H), 3.21 – 2.86 (2m, 2H), 2.14 – 2.02 (m, 1H), 1.80 – 1.66 (m, 2H), 1.50 – 1.38 (m, 2H), 1.36 – 1.12 (m, 3H), 1.17 (t, J = 7.1 Hz, 3H); ^{13}C NMR (75 MHz, DMSO-d_6) δ 157.3, 154.7, 147.0 (d, J = 1.5 Hz), 140.7, 128.8, 121.0, 120.2 (q, J = 256.0 Hz), 70.7, 60.6, 59.3, 42.6, 42.2, 42.1, 39.2, 38.3, 33.6, 28.9, 14.7; HRMS (ESI) m/z calcd for $C_{21}H_{29}F_3N_3O_5$ [M+H$^+$] 460.1981, found 460.2040.

4.2.5.11. *N,N*-Dimethyl-4-[({[4-(trifluoromethoxy)benzyl]amino}carbonyl)amino]-1-oxa-9-azaspiro[5.5]undecane-9-carboxamide (20)

Yield 184 mg (69.4%), clear oil. ^{1}H NMR (300 MHz, DMSO-d_6) δ 7.38 – 7.26 (m, 4H), 6.31 (t, J = 6.0 Hz, 1H), 5.89 (d, J = 7.8 Hz, 1H), 4.21 (d, J = 6.0 Hz, 2H), 3.82 – 3.49 (m, 3H), 3.26 – 3.15 (m, 2H), 3.10 – 2.80 (2m, 2H), 2.70 (s, 6H), 2.10 – 1.99 (m, 1H), 1.79 – 1.67 (m, 2H), 1.56 – 1.14 (m, 5H); ^{13}C NMR (75 MHz, DMSO-d_6) δ 164.0, 157.3, 147.0 (q, J = 1.7 Hz), 140.7, 128.8, 120.9, 120.1 (q, J = 255.8 Hz), 71.0, 59.2, 42.7, 42.2, 42.1, 42.0, 41.9, 38.5, 38.2, 33.6, 29.1; HRMS (ESI) m/z calcd for $C_{21}H_{30}F_3N_4O_4$ [M+H$^+$] 459.2141, found 459.2216.

4.2.5.12. *N*-[9-(Ethylsulfonyl)-1-oxa-9-azaspiro[5.5]undec-4-yl]-*N'*-[4-(trifluoromethoxy)-benzyl]urea (21)

Yield 235 mg (84.7%), clear oil. ^{1}H NMR (400 MHz, DMSO-d_6) δ 7.39 – 7.26 (m, 4H), 6.31 (t, J = 6.0 Hz, 1H), 5.90 (d, J = 7.9 Hz, 1H), 4.21 (d, J = 6.0 Hz, 2H), 3.81 – 3.63 (m, 2H), 3.59 – 3.49 (m, 1H), 3.31 – 3.26 (m, 2H), 3.11 – 3.03 (m, 1H), 3.02 (q, J = 7.3 Hz, 2H), 2.94 – 2.84 (m, 1H), 2.25 – 2.16 (m, 1H), 1.78 – 1.68 (m, 2H), 1.63 – 1.48 (m, 2H), 1.44 – 1.32 (m, 1H), 1.29 – 1.05 (m, 2H), 1.19 (t, J = 7.3 Hz, 3H); ^{13}C NMR (75 MHz, DMSO-d_6) δ 158.9, 148.6 (d, J = 1.6 Hz), 142.2, 130.4, 122.5, 121.7 (q, J = 255.5 Hz), 71.6, 60.8, 44.1, 43.9, 43.7 (d, J = 4.4 Hz), 42.6 (d, J = 4.4 Hz), 39.8, 35.1, 30.5, 9.1; HRMS (ESI) m/z calcd for $C_{20}H_{29}F_3N_3O_4S$ [M+H$^+$] 480.1702, found 480.1175.

4.2.5.13. *N*-[9-(Isopropylsulfonyl)-1-oxa-9-azaspiro[5.5]undec-4-yl]-*N'*-[4-(trifluoro-methoxy)benzyl]urea (22)

Yield 246 mg (86.2%), clear oil. ^{1}H NMR (400 MHz, DMSO-d_6) δ 7.40 – 7.25 (m, 4H), 6.30 (t, J = 5.9 Hz, 1H), 5.89 (d, J = 7.7 Hz, 1H), 4.21 (d, J = 5.9 Hz, 2H), 3.80 – 3.62 (m, 2H), 3.59 – 3.49 (m, 1H), 3.41 – 3.25 (m, 3H), 3.19 – 3.10 (m, 1H), 3.02 – 2.93 (m, 1H), 2.22 – 2.13 (m,

1H), 1.77 – 1.69 (m, 2H), 1.60 – 1.46 (m, 2H), 1.41 – 1.04 (m, 3H), 1.20 (d, J = 6.8 Hz, 6H); ^{13}C NMR (75 MHz, DMSO-d_6) δ 157.3, 147.0 (d, J = 1.6 Hz), 140.7, 128.8, 120.9, 120.1 (q, J = 255.7 Hz), 70.20, 59.2, 51.7, 42.6, 42.1, 42.0, 41.4, 41.3, 38.7, 33.5, 29.4, 16.5; HRMS (ESI) m/z calcd for $C_{21}H_{31}F_3N_3O_5S$ [M+H$^+$] 494.1858, found 494.1969.

4.2.5.14.   *N*-Propyl-4-[({[4-(trifluoromethoxy)benzyl]amino}carbonyl)amino]-1-oxa-9-azaspiro[5.5]undecane-9-carboxamide (23)

Yield 198 mg (72.3%), white solid, m.p. 174-176 °C. ^{1}H NMR (300 MHz, DMSO-d_6) δ 7.40 – 7.25 (m, 4H), 6.40 (t, J = 5.3 Hz, 1H), 6.31 (t, J = 5.9 Hz, 1H), 5.89 (d, J = 7.6 Hz, 1H), 4.21 (d, J = 5.9 Hz, 2H), 3.83 – 3.46 (m, 5H), 3.10 – 2.80 (m, 4H), 2.06 – 1.93 (m, 1H), 1.78 – 1.66 (m, 2H), 1.48 – 1.12 (m, 7H), 0.80 (t, J = 7.6 Hz, 3H); ^{13}C NMR (75 MHz, DMSO-d_6) δ 157.4, 157.3, 147.0, 140.6, 128.8, 120.9, 120.1 (q, J = 255.7 Hz), 70.9, 59.2, 42.6, 42.1, 41.9, 39.1, 38.5, 33.6, 29.1, 23.1, 11.4; HRMS (ESI) m/z calcd for $C_{22}H_{32}F_3N_4O_4$ [M+H$^+$] 473.2297, found 473.2356.

4.2.5.15. Methyl 4-oxo-4-{4-[({[4-(trifluoromethoxy)benzyl]amino}carbonyl)amino]-1-oxa-9-azaspiro[5.5]undec-9-yl}butanoate (24)

Yield 227 mg (78.3%), white solid, m.p. 101-103 °C. ^{1}H NMR (400 MHz, DMSO-d_6) δ 7.39 – 7.26 (m, 4H), 6.36 (t, J = 5.9 Hz, 1H), 5.94 (d, J = 8.0 Hz, 1H), 4.21 (d, J = 5.9 Hz, 2H), 4.00 – 3.90 (m, 1H), 3.81 – 3.64 (m, 2H), 3.61 – 3.50 (m, 2H), 3.57 (s, 3H), 3.20 – 2.73 (3m, 2H), 2.59 – 2.53 (m, 2H), 2.49 – 2.43 (m, 2H), 2.17 – 2.03 (m, 1H), 1.79 – 1.67 (m, 2H), 1.58 – 1.04 (m, 5H); ^{13}C NMR (75 MHz, DMSO-d_6) δ 173.1, 169.0, 157.4, 147.0 (q, J = 1.7 Hz), 140.7, 128.8, 120.9, 120.1 (q, J = 255.8 Hz), 70.9, 59.4, 59.3, 51.3, 42.7, 42.6, 42.1, 40.5, 38.9, 38.3, 37.0, 36.9, 33.6, 28.8, 27.4; HRMS (ESI) m/z calcd for $C_{23}H_{31}F_3N_3O_6$ [M+H$^+$] 502.2087, found 502.2136.

4.2.5.16.   *N*-[9-(Methylsulfonyl)-1-oxa-9-azaspiro[5.5]undec-4-yl]-*N'*-[4-(trifluoromethyl)-benzyl]urea (25)

Yield 91 mg (35.1%), white solid, m.p. 176-178 °C. ^{1}H NMR (300 MHz, DMSO-d_6) δ 7.63 – 7.49 (m, 2H), 7.45 – 7.32 (m, 2H), 4.37 (s, 2H), 4.03 – 3.86 (m, 1H), 3.81 – 3.68 (m, 1H), 3.63 – 3.39 (m, 3H), 3.11 – 2.94 (m, 1H), 2.91 – 2.70 (m, 1H), 2.76 (s, 3H), 2.35 – 2.18 (m, 1H), 1.96 – 1.73 (m, 2H), 1.71 – 1.55 (m, 2H), 1.53 – 1.08 (m, 3H); ^{13}C NMR (75 MHz, DMSO-d_6) δ 157.3, 146.2, 127.6, 127.2 (q, J = 31.5 Hz), 125.1 (q, J = 3.7 Hz), 124.5 (q, J = 271.9 Hz), 69.9, 59.3, 42.6, 42.5, 42.1, 41.3, 41.2, 37.9, 33.7, 33.5, 28.5; HRMS (ESI) m/z calcd for $C_{19}H_{27}F_3N_3O_4S$ [M+H$^+$] 450.1596, found 450.1669.

4.2.5.17. *N*-(4-Chlorobenzyl)-*N′*-[9-(methylsulfonyl)-1-oxa-9-azaspiro[5.5]undec-4-yl]urea (26)

Yield 75 mg (31%), clear oil. ^{1}H NMR (300 MHz, CDCl$_3$) δ 7.33 – 7.13 (m, 4H), 4.29 (s, 2H), 4.03 – 3.86 (m, 1H), 3.81 – 3.69 (m, 1H), 3.62 – 3.42 (m, 3H), 3.11 – 2.95 (m, 1H), 2.90 – 2.71 (m, 1H), 2.76 (s, 3H), 2.37 – 2.21 (m, 1H), 1.98 – 1.73 (m, 2H), 1.72 – 1.55 (m, 2H), 1.54 – 1.39 (m, 1H), 1.38 – 1.08 (m, 2H); ^{13}C NMR (75 MHz, CDCl$_3$) δ 157.7, 137.6, 133.3, 129.0, 128.9, 70.4, 59.9, 43.9, 43.5, 43.2, 41.6, 41.4, 38.7, 34.5, 33.7, 29.3; HRMS (ESI) *m/z* calcd for C$_{18}$H$_{27}$ClN$_3$O$_4$S [M+H$^+$] 416.1332, found 416.1405.

4.2.5.18. *N*-[9-(Methylsulfonyl)-1-oxa-9-azaspiro[5.5]undec-4-yl]-*N′*-[4-(methylthio)benzyl]-urea (27)

Yield – 83 mg (33.4%), clear oil. ^{1}H NMR (400 MHz, DMSO-*d$_6$*) δ 7.24 – 7.14 (m, 4H), 6.20 (t, *J* = 6.0 Hz, 1H), 5.84 (d, *J* = 7.8 Hz, 1H), 4.14 (d, *J* = 6.0 Hz, 2H), 3.82 – 3.63 (m, 2H), 3.59 – 3.50 (m, 1H), 3.30 – 3.22 (m, 2H), 3.03 – 2.92 (m, 1H), 2.86 – 2.76 (m, 1H), 2.84 (s, 3H), 2.44 (s, 3H), 2.28 – 2.19 (m, 1H), 1.78 – 1.69 (m, 2H), 1.66 – 1.50 (m, 2H), 1.46 – 1.36 (m, 1H), 1.29 – 1.05 (m, 2H); ^{13}C NMR (75 MHz, DMSO-*d$_6$*) δ 157.3, 137.8, 136.0, 127.8, 126.1, 69.8, 59.3, 42.6, 42.4, 42.0, 41.2, 41.1, 37.9, 33.8, 33.6, 28.5, 15.1. HRMS (ESI) *m/z* calcd for C$_{19}$H$_{30}$N$_3$O$_4$S$_2$ [M+H$^+$] 428.1599, found 428.1672.

4.2.5.19. *N*-(4-Bromobenzyl)-*N′*-[9-(methylsulfonyl)-1-oxa-9-azaspiro[5.5]undec-4-yl]urea (28)

Yield – 83 mg (31.1%), white solid, m.p. 141-143 °C. ^{1}H NMR (300 MHz, DMSO-*d$_6$*) δ 7.54 – 7.45 (m, 2H), 7.24 – 7.15 (m, 2H), 6.29 (t, *J* = 5.9 Hz, 1H), 5.90 (d, *J* = 7.8 Hz, 1H), 4.15 (d, *J* = 5.9 Hz, 2H), 3.82 – 3.47 (m, 3H), 3.32 – 3.21 (m, 2H), 3.04 – 2.90 (m, 1H), 2.88 – 2.73 (m, 1H), 2.84 (s, 3H), 2.31 – 2.18 (m, 1H), 1.80 – 1.67 (m, 2H), 1.66 – 1.48 (m, 2H), 1.46 – 1.05 (m, 3H); ^{13}C NMR (75 MHz, DMSO-*d$_6$*) δ 157.3, 140.6, 131.1, 129.3, 119.5, 69.8, 59.2, 42.5, 42.2, 42.1, 41.2, 41.1, 37.9, 33.7, 33.6, 28.5; HRMS (ESI) *m/z* calcd for C$_{18}$H$_{26}$BrN$_3$O$_4$SNa [M+Na$^+$] 482.0719, found 482.0720.

4.2.5.20. *N*-[4-(Diethylamino)benzyl]-*N′*-[9-(methylsulfonyl)-1-oxa-9-azaspiro[5.5]undec-4-yl]urea (29)

Yield 91 mg (34.8%), white solid, m.p. 132-133 °C. ^{1}H NMR (400 MHz, DMSO-*d$_6$*) δ 7.05 – 6.99 (m, 2H), 6.62 – 6.56 (m, 2H), 5.99 (t, *J* = 5.6 Hz, 1H), 5.73 (d, *J* = 7.8 Hz, 1H), 4.03 (d, *J* = 5.6 Hz, 2H), 3.81 – 3.62 (m, 2H), 3.59 – 3.50 (m, 1H), 3.30 – 3.22 (m, 6H), 3.03 – 2.92 (m, 1H), 2.86 – 2.77 (m, 1H), 2.84 (s, 3H), 2.28 – 2.19 (m, 1H), 1.78 – 1.69 (m, 2H), 1.66 – 1.50 (m, 2H),

1.47 – 1.38 (m, 1H), 1.27 – 1.04 (m, 2H), 1.05 (t, J = 7.0 Hz, 6H); ^{13}C NMR (75 MHz, DMSO-d_6) δ 158.8, 147.9, 130.0, 128.5, 113.2, 71.4, 60.8, 45.3, 44.2, 44.1, 43.5, 42.8, 42.7, 39.4, 35.3, 35.2, 30.1, 13.9; HRMS (ESI) m/z calcd for $C_{22}H_{37}N_4O_4S$ [M+H$^+$] 453.2457, found 453.2540.

4.2.5.21. *N*-Benzyl-*N′*-[9-(methylsulfonyl)-1-oxa-9-azaspiro[5.5]undec-4-yl]urea (30)

Yield – 85 mg (38.5%), white solid, m.p. 180-182 °C. ^{1}H NMR (300 MHz, DMSO-d_6) δ 7.37 – 7.16 (m, 5H), 6.23 (t, J = 5.8 Hz, 1H), 5.84 (d, J = 7.7 Hz, 1H), 4.19 (d, J = 5.8 Hz, 2H), 3.86 – 3.62 (m, 2H), 3.61 – 3.48 (m, 1H), 3.29 – 3.21 (m, 2H), 3.05 – 2.90 (m, 1H), 2.87 – 2.73 (m, 1H), 2.84 (s, 3H), 2.30 – 2.18 (m, 1H), 1.82 – 1.69 (m, 2H), 1.68 – 1.49 (m, 2H), 1.48 – 1.39 (m, 1H), 1.32 – 1.04 (m, 2H); ^{13}C NMR (75 MHz, DMSO-d_6) δ 157.3, 140.9, 128.2, 127.0, 126.6, 69.8, 59.3, 42.8, 42.6, 42.0, 41.2, 41.2, 37.9, 33.7, 33.6, 28.5; HRMS (ESI) m/z calcd for $C_{18}H_{28}N_3O_4S$ [M+H$^+$] 382.1722, found 382.1795.

4.2.5.22. *N*-(4-Methylbenzyl)-*N′*-[9-(methylsulfonyl)-1-oxa-9-azaspiro[5.5]undec-4-yl]urea (31)

Yield – 100 mg (42.7%), white solid, m.p. 141-143 °C. ^{1}H NMR (300 MHz, DMSO-d_6) δ 7.15 – 7.06 (m, 4H), 6.17 (t, J = 5.9 Hz, 1H), 5.82 (d, J = 7.8 Hz, 1H), 4.14 (d, J = 5.9 Hz, 2H), 3.83 – 3.61 (m, 2H), 3.60 – 3.47 (m, 1H), 3.31 – 3.20 (m, 2H), 3.04 – 2.91 (m, 1H), 2.86 – 2.74 (m, 1H), 2.84 (s, 3H), 2.29 – 2.19 (m, 1H), 2.26 (s, 3H), 1.80 – 1.69 (m, 2H), 1.67 – 1.34 (m, 3H), 1.30 – 1.02 (m, 2H); ^{13}C NMR (75 MHz, DMSO-d_6) δ 157.3, 137.8, 135.6, 128.8, 127.0, 69.8, 59.2, 42.6, 42.5, 42.0, 41.2, 41.2, 37.9, 33.8, 33.6, 28.5, 20.7; HRMS (ESI) m/z calcd for $C_{19}H_{30}N_3O_4S$ [M+H$^+$] 396.1879, found 396.1952.

4.2.5.23. *N,N*-Dimethyl-4-(3-(4-(trifluoromethoxy)benzyl)ureido)-1-oxa-9-azaspiro[5.5]un-decane-9-sulfonamide (32)

Yield – 152 mg (53.2%), clear oil. ^{1}H NMR (300 MHz, DMSO-d_6) δ 7.39 – 7.27 (m, 4H), 6.33 (br s, 1H), 5.90 (br s, 1H), 4.26 – 4.18 (m, 2H), 3.81 – 3.63 (m, 3H), 3.32 – 3.22 (m, 2H), 3.14 – 3.02 (m, 1H), 2.97 – 2.85 (m, 1H), 2.73 (s, 6H), 2.24 – 2.13 (m, 1H), 1.77 – 1.68 (m, 2H), 1.62 – 1.18 (m, 5H); ^{13}C NMR (75 MHz, DMSO-d_6) δ 157.3, 147.0 (d, J = 1.7 Hz), 140.7, 128.8, 120.9, 120.1 (q, J = 255.7 Hz), 70.1, 59.2, 42.6, 42.1, 42.0, 41.8, 41.7, 38.1, 37.9, 33.5, 28.8; HRMS (ESI) m/z calcd for $C_{20}H_{30}F_3N_4O_5S$ [M+H$^+$] 495.1883, found 495.1884.

4.2.6. General procedure for preparation of compounds 33-45.

9-Benzyl-1-oxa-9-azaspiro[5.5]undecan-4-amine (**7**, 156 mg, 0.60 mmol) was dissolved in diethyl ether (8 mL) and treated with the respective isocyanate (0.63 mL, added dropwise). The

resulting mixture was stirred overnight. The precipitate formed was separated by filtration, washed with diethyl ether and dried in vacuo to provide the title compound.

4.2.6.1. *N*-(9-benzyl-1-oxa-9-azaspiro[5.5]undec-4-yl)-*N′*-(3-fluoro-4-methylphenyl)urea (33)

Yield – 76 mg (31.1%), white solid, m.p. 228-230 °C. ^{1}H NMR (300 MHz, DMSO-d_6) δ 8.84 (s, 0.9H), 7.67 – 7.56 (m, 2H), 7.52 – 7.42 (m, 3H), 7.41 – 7.32 (m, 1H), 7.29 – 7.02 (m, 2H), 6.96 – 6.85 (m, 1H), 6.47 – 6.34 (m, 1H), 4.42 – 4.23 (m, 2H), 3.90 – 3.66 (m, 2H), 3.64 – 3.49 (m, 1H), 3.21 – 3.01 (m, 3H), 3.00 – 2.77 (m, 1H), 2.48 – 2.41 (m, 1H), 2.29 (s, 1H), 2.11 (s, 3H), 2.02 – 1.85 (m, 1H), 1.82 – 1.59 (m, 3H), 1.40 – 1.04 (m, 2H); ^{13}C NMR (75 MHz, DMSO-d_6) δ 160.6 (d, *J* = 239.9 Hz), 154.6, 140.0 (d, *J* = 11.3 Hz), 131.4 (d, *J* = 7.4 Hz), 129.7, 129.0, 116.1 (d, *J* = 17.5 Hz), 113.4 (d, *J* = 2.7 Hz), 104.5 (d, *J* = 27.2 Hz), 78.2, 68.8, 59.7, 47.20, 47.1, 42.1, 32.9, 26.2, 13.6 (d, *J* = 2.6 Hz); HRMS (ESI) *m/z* calcd for $C_{24}H_{31}FN_3O_2$ [M+H$^+$] 412.2322, found 412.2405.

4.2.6.2. *N*-(9-Benzyl-1-oxa-9-azaspiro[5.5]undec-4-yl)-*N′*-(5-chloro-2-methoxyphenyl)urea (34)

Yield – 128 mg (48.1%), white solid, m.p. 154-156 °C. ^{1}H NMR (300 MHz, DMSO-d_6) δ 8.23 – 8.15 (m, 1H), 7.99 (s, 1H), 7.36 – 7.20 (m, 5H), 7.02 – 6.85 (m, 3H), 3.86 – 3.72 (m, 4H), 3.68 – 3.57 (m, 2H), 3.52 – 3.44 (m, 2H), 2.47 – 2.32 (m, 3H), 2.29 – 2.16 (m, 1H), 2.13 – 2.00 (m, 1H), 1.86 – 1.71 (m, 2H), 1.63 – 1.36 (m, 3H), 1.32 – 1.14 (m, 1H), 1.05 (t, J = 12.1 Hz, 1H). ^{13}C NMR (75 MHz, DMSO-d_6) δ 154.7, 146.4, 137.7, 130.9, 129.7, 128.6, 127.6, 124.7, 120.6, 117.4, 112.2, 70.8, 62.3, 59.2, 56.4, 48.6, 48.5, 42.5, 38.5, 33.4, 29.1; HRMS (ESI) *m/z* calcd for $C_{24}H_{31}ClN_3O_3$[M+H$^+$] 444.1976, found 444.2037.

4.2.6.3. *N*-(9-Benzyl-1-oxa-9-azaspiro[5.5]undec-4-yl)-*N′*-(3-fluoro-4-methoxyphenyl)urea (35)

Yield – 153 mg (59.7%), white solid, m.p. 179-181 °C, yield 60 %; ^{1}H NMR (300 MHz, DMSO-d_6) δ 8.30 (s, 1H), 7.41 (dd, *J* = 14.1, 2.3 Hz, 1H), 7.34 – 7.19 (m, 5H), 7.06 – 6.91 (m, 2H), 6.00 (d, *J* = 7.7 Hz, 1H), 3.85 – 3.73 (m, 4H), 3.68 – 3.49 (m, 2H), 3.44 (s, 2H), 2.47 – 2.25 (m, 3H), 2.23 – 2.11 (m, 1H), 2.10 – 1.99 (m, 1H), 1.80 – 1.69 (m, 2H), 1.60 – 1.35 (m, 3H), 1.33 – 1.17 (m, 1H), 1.14 – 1.03 (m, 1H); ^{13}C NMR (75 MHz, DMSO-d_6) δ 154.7, 151.4 (d, *J* = 241.1 Hz), 141.6 (d, *J* = 10.8 Hz), 138.6, 134.2 (d, *J* = 9.8 Hz), 129.1, 128.3, 127.0, 114.6 (d, *J* = 2.7 Hz), 113.7 (d, *J* = 3.3 Hz), 106.6 (d, *J* = 22.7 Hz), 70.7, 62.4, 59.0, 56.5, 48.6, 48.5, 42.5, 42.3, 38.8, 33.4, 29.3; HRMS (ESI) *m/z* calcd for $C_{24}H_{31}FN_3O_3$[M+H$^+$] 428.2271, found 428.2363.

4.2.6.4. *N*-(9-benzyl-1-oxa-9-azaspiro[5.5]undec-4-yl)-*N′*-(3-chlorophenyl)urea (36)

Yield – 76 mg (30.9%), white solid, m.p. 59-61 °C. ^{1}H NMR (300 MHz, DMSO-d_6) δ 8.54 (s, 1H), 7.65 (s, 1H), 7.36 – 7.11 (m, 7H), 6.96 – 6.88 (m, 1H), 6.14 (d, *J* = 7.5 Hz, 1H), 3.86 – 3.72 (m, 1H), 3.68 – 3.54 (m, 2H), 3.45 (s, 2H), 2.47 – 2.27 (m, 3H), 2.24 – 2.12 (m, 1H), 2.10 – 2.00 (m, 1H), 1.82 – 1.71 (m, 2H), 1.61 – 1.36 (m, 3H), 1.34 – 1.21 (m, 1H), 1.17 – 1.04 (m, 1H); ^{13}C NMR (75 MHz, DMSO-d_6) δ 154.5, 142.1, 138.6, 133.3, 130.5, 129.1, 128.3, 127.1, 120.9, 117.2, 116.3, 70.8, 62.5, 59.0, 48.6, 48.5, 42.4, 38.9, 33.3, 29.3; HRMS (ESI) *m/z* calcd for $C_{23}H_{28}ClN_3O_2Na$ [M+Na$^+$] 436.1768, found 436.1762.

4.2.6.5. *N*-(9-Benzyl-1-oxa-9-azaspiro[5.5]undec-4-yl)-*N′*-(3-chloro-4-fluorophenyl)urea (37)

Yield – 163 mg (63.2%), white solid, m.p. 69-71 °C. ^{1}H NMR (300 MHz, DMSO-d_6) δ 8.54 (s, 1H), δ 7.78 – 7.72 (m, 1H), 7.35 – 7.14 (m, 7H), 6.15 (d, *J* = 7.6 Hz, 1H), 3.87 – 3.71 (m, 1H), 3.68 – 3.49 (m, 2H), 3.43 (s, 2H), 2.47 – 2.25 (m, 3H), 2.23 – 2.11 (m, 1H), 2.10 – 1.99 (m, 1H), 1.81 – 1.70 (m, 2H), 1.60 – 1.35 (m, 3H), 1.34 – 1.19 (m, 1H), 1.16 – 1.05 (m, 1H); ^{13}C NMR (75 MHz, DMSO-d_6) δ 154.4, 151.9 (d, *J* = 239.8 Hz), 138.6, 137.8 (d, *J* = 2.7 Hz), 128.9, 128.1, 126.8, 119.1, 118.9, 117.8 (d, *J* = 6.6 Hz), 116.7 (d, *J* = 21.6 Hz), 70.6, 62.3, 58.8, 48.5, 48.4, 42.3, 38.8, 33.2, 29.3; HRMS (ESI) *m/z* calcd for $C_{23}H_{28}ClFN_3O_2$ [M+H$^+$] 432.1776, found 432.1860.

4.2.6.6. *N*-(9-Benzyl-1-oxa-9-azaspiro[5.5]undec-4-yl)-*N′*-(4-fluorophenyl)urea (38)

Yield – 166 mg (69.9%), white solid, m.p. 166-168 °C. ^{1}H NMR (300 MHz, DMSO-d_6) δ 8.32 (s, 1H), 7.44 – 7.18 (m, 7H), 7.11 – 6.98 (m, 2H), 6.00 (d, *J* = 7.5 Hz, 1H), 3.88 – 3.71 (m, 1H), 3.68 – 3.49 (m, 2H), 3.43 (s, 2H), 2.47 – 2.26 (m, 3H), 2.24 – 2.12 (m, 1H), 2.10 – 1.99 (m, 1H), 1.82 – 1.71 (m, 2H), 1.60 – 1.36 (m, 3H), 1.34 – 1.17 (m, 1H), 1.15 – 1.03 (m, 1H). ^{13}C NMR (75 MHz, DMSO-d_6) δ 157.5 (d, *J* = 237.4 Hz), 155.2, 138.5, 136.9 (d, *J* = 2.3 Hz), 129.6, 128.6, 127.4, 120.1 (d, *J* = 7.6 Hz), 115.6 (d, *J* = 22.1 Hz), 71.1, 62.7, 59.3, 48.8, 48.7, 42.6, 38.9, 33.6, 29.4; HRMS (ESI) *m/z* calcd for $C_{23}H_{29}FN_3O_2$ [M+H$^+$] 398.2165, found 398.2228.

4.2.6.7. *N*-(9-Benzyl-1-oxa-9-azaspiro[5.5]undec-4-yl)-*N′*-[4-(trifluoromethoxy)benzyl]urea (39)

Yield 239 mg (83.6%), clear oil. ^{1}H NMR (300 MHz, DMSO-d_6) δ 7.39 – 7.19 (m, 9H), 6.30 (t, *J* = 5.9 Hz, 1H), 5.88 (d, *J* = 7.8 Hz, 1H), 4.20 (d, *J* = 5.9 Hz, 2H), 3.79 – 3.66 (m, 1H), 3.65 – 3.46 (m, 2H), 3.42 (s, 2H), 2.46 – 2.24 (m, 3H), 2.21 – 2,10 (m, 1H), 2.06 – 1.98 (m, 1H), 1.76 – 1.65 (m, 2H), 1.58 – 1.31 (m, 3H), 1.27 – 1.14 (m, 1H), 1.12 – 0.97 (m, 1H); ^{13}C NMR (75 MHz, DMSO-d_6) δ 157.4, 148.6 (q, *J* = 1.9 Hz), 140.6, 138.5, 128.9, 128.8, 128.1, 126.9, 120.9, 120.15

(d, J = 255.9 Hz). 70.6, 62.3, 58.9, 48.5, 48.4, 42.7, 42.3, 42.2, 38.8, 33.7, 29.2; HRMS (ESI) m/z calcd for $C_{25}H_{31} F_3N_3O_3$ [M+H$^+$] 478.2239, found 478.2339.

4.2.6.8. *N*-(9-benzyl-1-oxa-9-azaspiro[5.5]undec-4-yl)-*N'*-cyclohexylurea (40)

Yield – 198 mg (85.6%), white solid, m.p. 91-93 °C. ^{1}H NMR (300 MHz, CDCl$_3$) δ 7.35 – 7.17 (m, 5H), 5.63 – 5.49 (dd, J = 12.32 Hz, J =12.11 Hz, 2H), 3.75 – 3.45 (m, 3H), 3.43 (s, 2H), 3.36 – 3.27 (m, 1H), 2.45 – 2.25 (m, 3H), 2.22 – 2.11 (m, 1H), 2.05 – 1.95 (m,1H), 1.78 – 1.56 (m, 6H), 1.55 – 1.34 (m, 4H), 1.30 – 0.94 (m, 7H); ^{13}C NMR (75 MHz, DMSO-d_6) δ 156.7, 138.6, 128.9, 128.2, 70.6, 62.4, 58.9, 48.6, 48.4, 47.67, 42.8, 42.0, 38.8, 33.8, 33.3, 29.3, 25.3, 24.5; HRMS (ESI) m/z calcd for $C_{23}H_{36}N_3O_2$ [M+H$^+$] 386.2729, found 386.2842.

4.2.6.9. *N*-(9-benzyl-1-oxa-9-azaspiro[5.5]undec-4-yl)-*N'*-ethylurea (41)

Yield – 178 mg (89.5%), white solid, m.p. 159-161 °C. ^{1}H NMR (300 MHz, DMSO-d_6) δ 7.35 – 7.18 (m, 5H), 5.68 – 5.59 (m, 2H), 3.77 – 3.45 (m, 3H), 3.43 (s, 2H), 3.05 – 2.92 (m, 2H), 2.45 – 2.25 (m, 3H), 2.23 – 2.10 (m, 1H), 2.07 – 1.94 (m, 1H), 1.76 – 1.63 (m 2H), 1.58 – 1.32 (m, 3H), 1.26 – 1.08 (m,1H), 1.06 – 0.91 (m, 4H); ^{13}C NMR (75 MHz, DMSO-d_6) δ 157.5, 138.7, 129.0, 128.2, 126.9, 70.7, 62.4, 59.0, 48.2, 48.5, 42.2, 38.9, 34.1, 33.8, 29.3, 15.8; HRMS (ESI) m/z calcd for $C_{19}H_{30}N_3O_2$ [M+H$^+$] 332.2260, found 332.2347.

4.2.6.10. N-(9-benzyl-1-oxa-9-azaspiro[5.5]undec-4-yl)-N'-phenylurea (42)

Yield – 198 mg (87.1%), white solid, m.p. 161-162 °C. ^{1}H NMR (300 MHz, DMSO-d_6) δ 8.28 (s, 1H), 7.45 – 7.11 (m, 9H), 6.96 – 6.79 (m, 1H), 6.01 (d, J = 7.5 Hz, 1H), 3.89 – 3.72 (m, 1H), 3.71 – 3.50 (m, 2H), 3.44 (s, 2H), 2.47 – 2.26 (m, 3H), 2.25 – 2.12 (m, 1H), 2.10 – 1.97 (m, 1H), 1.85 – 1.71 (m, 2H), 1.62 – 1.37 (m, 3H), 1.35 – 1.17 (m, 1H), 1.16 – 1.02 (m, 1H); ^{13}C NMR (75 MHz, DMSO-d_6) δ 154.6, 140.5, 138.7, 129.0, 128.8, 128.2, 126.9, 121.2, 117.8, 70.7, 62.4, 58.9, 48.6, 48.4, 42.6, 42.2, 38.8, 33.5, 29.3; HRMS (ESI) m/z calcd for $C_{23}H_{30}N_3O_2$ [M+H$^+$] 380.2260, found 380.2337.

4.2.6.11. *N*-1-Adamantyl-*N'*-(9-benzyl-1-oxa-9-azaspiro[5.5]undec-4-yl)urea (43)

Yield – 218 mg (83.3%), white solid, m.p. 190-192 °C. ^{1}H NMR (300 MHz, DMSO-d_6) δ 7.37 – 7.17 (m, 5H), 5.52 (d, J = 7.6 Hz, 1H), 5.39 (s, 1H), 3.71 – 3.37 (m, 5H), 2.44 – 2.23 (m, 3H), 2.22 – 2.09 (m, 1H), 2.06 – 1.92 (m, 4H), 1.87 – 1.80 (m, 6H), 1.73 – 1.32 (m, 11H), 1.20 – 1.03 (m, 1H), 0.95 (t, J = 12.3 Hz, 1H); ^{13}C NMR (75 MHz, DMSO-d_6) δ 156.3, 138.6, 128.8, 128.1, 126.8, 70.5, 62.3, 58.9, 49.4, 48.5, 48.4, 42.90, 42.1, 41.6, 38.8, 36.1, 33.8, 29.3, 28.9; HRMS (ESI) m/z calcd for $C_{27}H_{40}N_3O_2$ [M+H$^+$] 438.3004, found 438.3133.

4.2.6.12. *N*-(9-Benzyl-1-oxa-9-azaspiro[5.5]undec-4-yl)-*N′*-(2-fluorophenyl)urea (44)

Yield – 177 mg (74.2%), white solid, m.p. 167-169 °C. ^{1}H NMR (300 MHz, DMSO-d_6) δ 8.22 – 8.03 (m, 2H), 7.36 – 7.22 (m, 5H), 7.20 – 7,02 (m, 2H), 6.96 – 6.85 (m, 1H), 6.54 (d, J = 7.4 Hz, 1H), 3.89 – 3.72 (m,1H), 3.70 – 3.50 (m, 2H), 3.45 (s, 2H), 2.47 – 2.27 (m, 3H), 2.26 – 2.13 (m, 1H), 2.10 – 1.99 (m, 3H), 1.86 – 1.73 (m, 2H), 1.62 – 1.37 (m, 3H), 1.32 – 1.16 (m, 1H), 1.14 – 1.01 (m, 1H); 13C NMR (75 MHz, DMSO-d6) δ 151.85 (d, J = 240.5 Hz), 128.28 (d, J = 10.1 Hz), 124.54 (d, J = 3.3 Hz), 121.90 (d, J = 7.3 Hz), 120.46 (s), 114.95 (d, J = 18.9 Hz); HRMS (ESI) *m/z* calcd for $C_{23}H_{29}FN_3O_2$ [M+H$^+$] 398.2165, found 398.2254.

4.2.6.13. *N*-(9-Benzyl-1-oxa-9-azaspiro[5.5]undec-4-yl)-*N′*-(2,4-difluorophenyl)urea (45)

Yield – 229 mg (92%), white solid, m.p. 239-241 °C. ^{1}H NMR (300 MHz, DMSO-d_6) δ 10.82 (s, 1H), 8.37 – 8.25 (m, 1H), 8.12 – 7.96 (m, 1H), 7.70 – 7.56 (m, 2H), 7.52 – 7.35 (m, 3H), 7.29 – 7.15 (m, 1H), 7.03 – 6.91 (m, 1H), 6.87 – 6.72 (m, 1H), 4.43 – 4.23 (m, 2H), 3.89 – 3.65 (m, 2H), 3.63 – 3.52 (m, 1H), 3.22 – 3.01 (m, 3H), 2.98 – 2.80 (m, 1H), 2.47 – 2.11 (m, 1H), 2.08 – 1.89 (m, 1H), 1.86 – 1.61 (m, 4H), 1.38 – 1.04 (m, 2H); ^{13}C NMR (75 MHz, DMSO-d_6) δ 156.5 (dd, J = 240.2, 11.5 Hz), 154.5, 151.9 (dd, J = 244.5, 12.1 Hz), 131.6, 129.9, 129.7, 129.0, 124.8 (dd, J = 10.8, 3.4 Hz), 121.8 (dd, J = 9.7, 1.9 Hz), 111.0 (dd, J = 21.6, 3.2 Hz), 103.7 (dd, J = 26.8, 23.8 Hz), 68.8, 59.6, 59.0, 47.2, 47.1, 42.3, 42.1, 39.5, 35.3, 32.9, 26.2; HRMS (ESI) *m/z* calcd for $C_{23}H_{28}F_2N_3O_2$ [M+H$^+$] 416.2071, found 416.2155.

4.2.7. Soluble epoxide hydrolase inhibition assay.

The IC$_{50}$ values of the compounds were determined by a fluorescence-based assay system of 96-well format. Non-fluorescent PHOME (3-phenyl-cyano-(6-methoxy-2-naphthalenyl)methyl ester-2-oxirane-acetic acid) was used as the substrate, which can be hydrolyzed by the sEH to the fluorescent 6-methoxynaphtaldehyde.[26] The formation of the product was measured (λ_{em}= 330 nm, λ_{ex}= 465 nm) by a Tecan Infinite F200 Pro plate reader. Recombinant human sEH (2 μg/well) was dissolved in pH 7 bis-Tris buffer with 0.1 mg/ml BSA containing a final concentration of 0.01% Triton-X 100. 100 μl aliquots of protein were incubated with different concentrations of compounds (final DMSO concentration 1%) for 30 min at room temperature. 10 μl aliquots of substrate were added (to the final concentration 50 μM). The hydrolyzed substrate was measured for 30 min (one point every minute). A blank control (no protein and no compound) as well as a positive control (no compound) was carried out as well. All measurements were performed in triplicates.

4.2.8. Solubility measurements for racemic compounds 13, 22, 27 and 32.

DPBS buffer at pH 7.4 with 0.01% Tween was combined with 1% of a DMSO solution of the inquired compound in a 96-well transparent flat bottom microtiter plate. Precipitation of the compound was measured at 650 nm using a microplate reader (Infinite M200, Tecan Group Ltd., Crailsheim, Germany).

4.2.9. Log D$_{7.4}$ determination for compounds 13, 22, 27 and 32.

LogD$_{7.4}$ determination via HPLC was performed according to a modified protocol described in the literature[27-28] using a Shimadzu LC-20A Prominence HPLC and a Shimadzu LC-MS 2020 mass spectrometer system with electrospray ionization and alternating positive and negative ion quadrupole mass spectrometry and scanning m/z 100 – 800 every 0.07 seconds. The HPLC column was a MultoHigh 100 RP18 3μ (2 mm I.D., 100 mm length, 3 μM particle size) from CS-Chromatographie Service GmbH (Langerwehe, Germany). A linear mobile phase gradient was used with mobile phase A as 100% acetonitrile, and mobile phase B as 100% 10mM ammonium acetate (adjusted to pH 7.4 with ammonium hydroxide and acetic acid). The gradient table was: 0 min/ 5% A, 2.0 min/ 5% A, 12.0 min/ 95% A, 20 min/ 95% A, 20.2 min/ 5% A, 25 min/ 5% A. Flowrate was 0.2 ml/min, and UV spectra were collected by 254 nm and 280 nm. The samples were dissolved in DMSO at 1 mg/ml and 1 to 5 μL were injected. The LogD$_{7.4}$ was calibrated to t$_R$ by running 23 reference compounds and plotting t$_R$ versus LogD$_{7.4}$ from the literature.[29] All determinations were performed in triplicates.

4.2.10. Enantiomer separation for compound (±)-22.

Chiral chromatography was performed using Shimadzu LC-10 high-performance liquid chromatography setup. The analytical work to confirm enantiomer separation was performed on Phenomenex 5x45 mm - 3 μ, amylose-2 column using 80:20 hexane-ethanol (1 mL/min at 25 ºC) as eluent and UV/CD 240 nm detector. Preparative enantiomer separation was performed on Phenomenex 25x250 mm - 3 μ, amylose-2 column using 80:20 hexane-ethanol (1 mL/min at 25 ºC) as eluent and UV/CD 240 nm detector.

(+)-22: $[\alpha]^{20}_D$ = +4.59 ± 0.56 ° (n = 3, l = 5.0 cm, c = 1.00 g/100 mL).

(−)-22: $[\alpha]^{20}_D$ = −1.39 ± 0.29 ° (n = 3, l = 5.0 cm, c = 1.00 g/100 mL).

4.2.11. Assignment of absolute configuration to (+)-22.

Quantum chemical investigations have been conducted at the Density Functional Theory (DFT) level of theory (B3LYP/6-31G*) by means of the Gaussian09 program suite.[30] To this end, the PDB-based crystal structure (PDB code 6FR2, cf. Figure 4) of the target compound (+)-22 was

utilized as initial structure for a constraint geometry optimization due to the otherwise high conformational flexibility of the molecular scaffold. Subsequent Time-Dependent Density Functional Theory (TDDFT) calculations gave rise to the excited state spectral properties and enantiomer-specific electronic circular dichroism (ECD) data. The bright states with high oscillator strengths around 180 nm are predominantly attributed to $\pi\pi^*$ transitions located at the phenyl moiety of (+)-**22**. The adjacent peak at 200 nm (which is of central importance for the ECD spectrum) corresponds to transitions in the geometric vicinity of the urea (carbamide) functionality with some orbital contribution at the stereocenter. Direct comparison to the experimental findings allows for unambiguous assignment of the S-configuration in accord with the abovementioned results. Implicit solvation effects (methanol) have been taken into account via the solvation model based on density (SMD) approach as implemented in Gaussian09.

4.2.12. Pharmacokinetic assessment of (±)-22.

4.2.12.1. Animals

Male JAXC57BL/6 J mice, supplied by the Laboratory Animal Centre (University of Eastern Finland, Kuopio, Finland), were housed in stainless steel cages and kept on a 12-h light/12-h dark cycle (lights on at 7:00 AM) at an ambient temperature of 22 ± 2 C and humidity $55 \pm 15\%$. Pelleted food (Teklad 2016S, Envigo, the Netherlands) and fresh tap water were available ad libitum. Animals were 8–10 weeks old and weighed 20 –27 g (n = 50). All experiments were performed in accordance with European Union guidelines (Directive 2010/63/EU and guidelines 2007/526/EC) and approved by the National Animal Experiment Board of Finland (project licence number ESAVI-2015-002090).

4.2.12.2. Analysis of the pharmacokinetics samples of compound (±)-22 by HPLC-MS.

Calibration standards were made in human serum at levels 0, 5, 10, 25, 50, 100, 250, 500, 1000, 1500, and 2000 ng/mL. The samples, calibration standards, and QC:s were processed by acetonitrile precipitation. First 400 μL of ice cold acetonitrile containing 0.5% formic acid and 200 ng/mL concentrations of internal standard (diclofenac) was mixed with serum samples (50 μL). The samples were vortex-mixed for approximately 10 seconds and centrifuged at 4500 rpm for 10 minutes at 4 ℃. The supernatant was recovered (200 μL) and transferred into HPLC vials.

The samples were analyzed using Agilent 1200 Series LC connected to Agilent 6410 Triple Quadrupole LC/MS (G6410A) with electrospray ion source (Agilent Technologies, Palo Alto, CA, USA). The separation was performed using a Zorbax SB-C18 column (2.1 x 50 mm, 2.7 μm), which was maintained at at 40 ℃. Injection volume was 2 μL. Eluent A was water and

eluent B methanol, both containing 0.1% (v/v) of formic acid. The gradient was as follows: 0 to 4 min: 30%→100% B, 4.0 to 5.0 min: 100% B, 5.0 to 5.1 min: 100→30% B, 5.1 to 7 min: 30% B. Flow rate was 0.4 mL/min. Total run time from injection to injection was 7.0 min.

Nitrogen was used as a drying, nebulizer, and collision gas. The following ion source conditions were employed: positive ion mode, drying gas temperature 300 ºC, drying gas flow 8 L/min, nebulizer pressure 40 psi. Multiple reaction monitoring (MRM) was used with both quadrupoles set at unit resolution. The mass transitions were m/z 494.2 > m/z 235.2 for the analyte and m/z 290.0 > m/z 250.0 for the internal standard, diclofenac. Agilent Masshunter quantitative analysis software was used for creating the calibration curves.

4.2.13. Cloning, expression and purification of *C*-terminal domain of sEH.

The cloning of the full-length sEH (sEH FL; aa1-aa555) construct was described previously.[31] The *C*-terminal sEH hydrolase domain (sEH Hyd) used in the crystallization experiment was cloned using the sEH FL construct as template. The sEH Hyd insert (aa222–aa555) was extracted and amplified by PCR (Primerfor: 3'-TTTCTCGAGCAACATCTTTGAGACCAC-5'; Primerrev: 3'-CGGGGTATTGAGGCTAGCCATATGTTT-5'). PCR products and pET24a(+) vector (with *C*-terminal hexa-His tag) were digested with XhoI and NdeI, before purified products were ligated by T4 DNA Ligase. Ligation products were amplified in DH5α cells and resulting plasmids were sequenced to ensure that there are no mutations in the protein sequence.

The expression and purification of the sEH-Hyd and sEH Fl were performed accordingly to a modified version of the purification protocol published by Hahn et al.[32] In brief, 1L ZYP5052 autoinduction media[33] was inoculated with 10 mL overnight culture of *E.coli* BL21-(DE3) cells either transformed with sEH-Fl or sEH-Hyd plasmid. As selection marker kanamycin was added. Cultures were incubated at 37 °C and 180 rpm for 2 h, before transferred to a 16 °C shaker. The cells were harvested after 36 h by centrifugation. Cell pellets were stored at -20 °C.

Bacterial pellets were thawed and re-suspended in buffer A (50 mM tris/HCl pH8, 500 mM NaCl, 70 mM imidazole/ HCl pH 7) with one tablet of Complete EDTA free protease inhibitor mix (Roche, Basel, Switzerland) and a trace amount of DNAse I (Applichem, Darmstadt, Germany). The re-suspended cells were lysed and cell debris were removed by centrifugation. The supernatant was purified by nickel affinity chromatography using a step gradient protocol. As running buffer A was used, while buffer B (identical to buffer A with an imidazole concentration of 400 mM) was used as elution buffer. The fractions containing the target protein were pooled. The sEH Fl was dialysed for 18-24 hours at 4°C against 100fold excess of buffer C (50 mM Tris, 50 mM NaCl, (HCl) pH 8) for activity assays using a 3500 kDa membrane. The

dialysis buffer was exchanged twice during the dialysis period. The protein samples intended for the use in assays were mix with glycerol to a final concentration of 20 % (v/v), before the concentration was determined by Nanodrop and aliquots were flash frozen in liquid nitrogen and stored at -80 °C. The sEH Hyd was concentrated 3fold by ultrafiltration to a final volume of 5 mL through 3000 Da cut-off membrane. The concentrated protein was applied onto the with buffer D (50 mM Tris/HCl pH 8, 500 mM NaCl) pre-equilibrated Superdex 75 HiLoad 16/600 column (GE Healthcare, Germany) and separated at the flow of 1 mL/min in the buffer D. sEH Hyd in buffer D was dialyzed in buffer E (50 mM NaCl, 50 mM sodium phosphate, 10 % (v/v) glycerol (98%), 2 mM DTT, pH 7.4) before concentrated by ultrafiltration (3000 Da cut-off membrane) to 5-10 mg/mL and flash frozen in liquid nitrogen. Frozen protein samples were stored at -80 °C.

4.2.14. Co-crystallization of (+)-22 with the *C*-terminal domain of sEH.

The *C*-terminal domain of sEH was crystalized according to Xing *et al.*[34] over the course of a month at 277 K by sitting-drop vapor diffusion. 1 μL of the protein solution (5-10 mg/mL, 50 mM NaCl, 50 mM sodium phosphate, 10% glycerol (98%), 2 mM DTT at pH 7.4 was mixed 1:1 with precipitant mixture (23 %-28 % (w/v) polyethylenglycol (PEG) 6000, 70 mM ammonium acetate, 200 mM magnesium acetate, 100 mM sodium cacodylate at pH 6.1-6.5). For soaking of the crystals, a saturated DMSO inhibitor solution of **(+)-22** was diluted 1:100 in PEG 400, before a second 1:9 dilution step in PEG 400/ precipitant mixture (3:7). Protein crystals where transferred into the soaking solution for 24 h, before the crystals were picked and flash frozen in the liquid nitrogen.

X-ray diffraction data of a single crystal was collected at the beamline station ID29 at the European Synchrotron Radiation Facility (ESRF), Grenoble, France. All diffraction data was obtained from a single crystal. The data was processed with XDS software package. The initial structure was obtained using the Phaser program[35] within PHENIX software package where polypeptide model from the PDB record 4JNC where coordinates for heteroatoms (water and ligands) were excluded from the starting model. After several iterative rounds of model building with Coot[36] and the model refinement using the PHENIX software package, a final value of R_{work} and R_{free}-factors of 0.168 and 0.210, respectively was reached. The graphical representations were made using MOE. Statistics of data collection and structural refinement are summarized in Table S1. The coordinates and structure-factor amplitudes of the structure have been deposited in the Protein Data Bank as entry 6FR2.

Acknowledgements

Supplementary data

Supplementary data associated with this article can be found, in the online version, at http://dx.doi.org/xxx.

References

1. Arand, M.; Grant, D. F.; Beetham, J. K.; Friedberg, T.; Oesch, F.; Hammock, B. D. *FEBS Lett.* **1994**, *338*, 251.

2. Oesch, F. *Xenobiotica* **1973**, *3*, 305.

3. Zeldin, D. C.; Kobayashi, J.; Falck, J. R.; Winder, B. S.; Hammock, B. D.; Snapper, J. R.; Capdevilla, J. H. *J. Biol. Chem.* **1993**, *268*, 6402

4. Spector, A. A.; Fang, X.; Snyder, G. D.; Weintraub, N. L. *Prog. Lipid Res.* **2004**, *43*, 55.

5. Fleming, I.; Rueben, A.; Popp, R.; Fisslthaler, B.; Schrodt, S.; Sander, A.; Haendeler, J.; Falck, J. R.; Morisseau, C.; Hammock, B. D.; Busse, R. Arterioscler. *Thromb. Vasc. Biol.* **2007**, *27*, 2612.

6. Imig, J. D. *Expert Opin. Drug Metab. Toxicol.* **2008**, *4*, 165.

7. Yu, Z.; Xu, F.; Huse, L. M.; Morisseau, C.; Draper, A. J.; Newman, J. W.; Parker, C.; Graham, L.; Engler, M. M.; Hammock, B. D.; Zeldin, D. C.; Kroetz, D. L. *Circ. Res.* **2000**, *87*, 992.

8. Spiecker, M.; Liao, J. K. *Arch. Biochem. Biophys.* **2005**, *433*, 420.

9. Imig, J. D.; Zhao, X.; Capdevilla, J. H.; Morisseau, C.; Hammock, B. D. *Hypertension* **2002**, *39*, 690.

10. Imig, J. D.; Zhao, X.; Zaharis, C. Z.; Olearczyk, J. J.; Pollock, D. M.; Newman, J. W.; Kim, I. H.; Watanabe, T.; Hammock, B. D. *Hypertension* **2005**, *46*, 975.

11. Gomez, G. A.; Morisseau, C.; Hammock, B. D.; Christianson, D. W. *Protein Sci.* **2006**, *15*, 58.

12. Morisseau, C.; Goodrow, M. H.; Dowdy, D.; Zheng, J.; Greene, J. F.; Sanborn, J. R.; Hammock, B. D. *Proc. Natl. Acad. Sci. U.S.A.* **1999**, *96*, 8849.

12. McElroy, N. R.; Jurs, P. C.; Morisseau, C.; Hammock, B. D. *J. Med. Chem.* **2003**, *46*, 1066.

13. Kim, I. H.; Morisseau, C.; Watanabe, T.; Hammock, B. D. *J. Med. Chem.* **2004**, *47*, 2110.

14. Kim, I. H.; Heirtzler, F. R.; Morisseau, C.; Nishi, K.; Tsai, H. J.; Hammock, B. D. *J. Med. Chem.* **2005**, *48*, 3621.

15. Schmelzer, K. R.; Kubala, L.; Newman, J. W.; Kim, I. H.; Eiserich, J. P.; Hammock, B. D. *Proc. Natl. Acad. Sci. U.S.A.* **2005**, *102*, 9772.

16. Burmistrov, V.; Morisseau, C.; Danilov, D.; Harris, T. R.; Dalinger, I.; Vatsadze, I.; Shkineva, T.; Butov, G. M.; Hammock, B. D. *Bioorg. Med. Chem. Lett.* **2015**, *25*, 5514.

17. Lovering, F.; Bikker, J.; Humblet, C. *J. Med. Chem.* **2009**, *52*, 6752-6756.

18. Kato, Y.; Fuchi, N.; Saburi, H.; Nishimura, Y.; Watanabe, A.; Yagi, M.; Nakadera, Y.; Higashi, E.; Yamada, M.; Aoki, T. *Bioorg. Med. Chem. Lett.* **2013**, *23*, 5975.

19. Kato, Y.; Fuchi, N.; Saburi, H.; Nishimura, Y.; Watanabe, A.; Yagi, M.; Nakadera, Y.; Higashi, E.; Yamada, M.; Aoki, T.; Kigoshi, H. *Bioorg. Med. Chem. Lett.* **2014**, *24*, 565.

20. Krasavin, M.; Lukin, A.; Bagnyukova, D.; Zhurilo, N.; Zahanich, I.; Zozulya, I.; Ihalainen, J.; Forsberg, M. M.; Lehtonen, M.; Rautio, J.; Moore, D.; Tikhonova, I. G. *Bioorg. Med. Chem.* **2016**, *24*, 5481.

21. (a) Lukin, A.; Bagnyukova, D.; Kalinchenkova, N.; Zhurilo, N.; Krasavin, M. *Tetrahedron Lett.* **2016**, *57*, 3311-3314; (b) Ghosh, A. K.; Shin, D.; Schilz, G. *Heterocycles* **2002**, *58*, 659-666.

22. Lee, K. S. S.; Liu, J.-Y.; Wagner, K. M.; Pakhomova, S.; Dong, H.; Morisseau, C.; Fu, S. H.; Yang, J.; Wang, P.; Ulu, A.; Mate, C. A.; Nguyen, L. V.; Hwang, S. H.; Edin, M. L.; Mara, A. A.; Wulff, H.; Newcomer, M. E.; Zeldin, D. C.; Hammock, B. D. *J. Med. Chem.* **2014**, *57*, 7016-7030.

23. Burmistrov, V.; Morisseau, C.; Lee, K. S. S.; Shihadih, D. S.; Harris, T. R.; Butov, G. M.; Hammock, B. D. *Bioorg. Med. Chem. Lett.* **2014**, *24*, 2193-2197.

24. Kim, I.-H.; Nishi, K.; Tsai, H.-J.; Bradford, T.; Koda, Y.; Watanabe, T.; Morisseau, C.; Blanchfield, J.; Toth, I.; Hammock, B. D. *Bioorg. Med. Chem.* **2007**, *15*, 312-313.

25. Fauber, B. P.; Rene, O.; de Leon Boenig, G.; Burton, B.; Deng, Y.; Eidenschenk, C.; Everett, C.; Gobbi, A.; Hymowitz, S. G.; Johnson, A. R.; La, H.; Liimatta, M.; Lockey, P.; Norman, M.; Ouyang, W.; Wang, W.; Wong, H. *Bioorg. Med. Chem. Lett.* **2014**, *24*, 3891-3897.

26. Wolf, N. M.; Morisseau, C.; Jones, P. D.; Hock, B.; Hammock, B. D. *Anal. Biochem.* **2006**, *355*, 71-80.

27. Chiang, P.-C.; Hu, Y. *Comb. Chem. High Throughput Screen*. **2009**, *12*, 250-257.

28. Kerns, E. H.; Di, L.; Petusky, S.; Kleintop, T.; Huryn, D.; McConnell, O.; Carter, G. *J. Chomatogr. B Analyt. Technol. Biomed. Life Sci.* **2003**, *791*, 381-388.

29. Büttner, D.; Kramer, J. S.; Klingler, F.-M.; Wittmann, S. K.; Hartmann, M. R.; Kurz, C. G.; Kohnhäuser, D.; Weizel, L.; Brüggerhoff, A.; Frank, D.; Steinhilber, D.; Wichelhaus, T. A.; Pogoryelov, D.; Proschak, E. *ACS Infect. Dis.* **2018**, DOI: 10.1021/acsinfecdis.7b00129.

30. Frisch, M. J.; Trucks, G. W.; Schlegel, H. B.; Scuseria, G. E.; Robb, M. A.; Cheeseman, J. R.; Scalmani, G.; Barone, V.; Mennucci, B.; Petersson, G. A.; Nakatsuji, H.; Caricato, M.; Li, X.; Hratchian, H. P.; Izmaylov, A. F.; Bloino, J.; Zheng, G.; Sonnenberg, J. L.; Hada, M.; Ehara, M.; Toyota, K.; Fukuda, R.; Hasegawa, J.; Ishida, M.; Nakajima, T.; Honda, Y.; Kitao, O.; Nakai, H.; Vreven, T.; Montgomery, J. A., Jr.; Peralta, J. E.; Ogliaro, F.; Bearpark, M.; Heyd, J. J.; Brothers, E.; Kudin, K. N.; Staroverov, V. N.; Keith, T.; Kobayashi, R.; Normand, J.; Raghavachari, K.; Rendell, A.; Burant, J. C.; Iyengar, S. S.; Tomasi, J.; Cossi, M.; Rega, N.; Millam, J. M.; Klene, M.; Knox, J. E.; Cross, J. B.; Bakken, V.; Adamo, C.; Jaramillo, J.; Gomperts, R.; Stratmann, R. E.; Yazyev, O.; Austin, A. J.; Cammi, R.; Pomelli, C.; Ochterski, J. W.; Martin, R. L.; Morokuma, K.; Zakrzewski, V. G.; Voth, G. A.; Salvador, P.; Dannenberg, J. J.; Dapprich, S.; Daniels, A. D.; Farkas, Ö.; Foresman, J. B.; Ortiz, J. V.; Cioslowski, J.; Fox, D. J. Gaussian, Inc., Wallingford CT, 2013.

31. Sandberg, M.; Hassett, C.; Adman, E. T.; Meijer, J.; Omiecinski, C. J. *J. Biol. Chem.* **2000**, *275*, 28873-28881.

32. Hahn, S.; Achenbach, J.; Buscató, E.; Klingler, F. M.; Schroeder, M.; Meirer, K.; Hieke, M.; Heering, J.; Barbosa-Sicard, E.; Loehr, F.; Fleming, I.; Doetsch, V.; Schubert-Zsilavecz, M.; Steinhilber, D.; Proschak, E. *ChemMedChem* **2011**, *6*, 2146-2149.

33. Studier, F. W. *Protein Expr. Purif.* **2005**, *41*, 207-234.

34. Xing, L.; McDonald, J. J.; Kolodziej, S. A.; Kurumbail, R. G.; Williams, J. M.; Warren, C. J.; O'Neal, J. M.; Skepner, J. E.; Roberds, S. L. *J. Med. Chem.* **2011**, *54*, 1211-1222.

35. McCoy, A.J.; Grosse-Kunstleve, R.W.; Adams, P.D.; Winn, M.D.; Storoni, L.C.; Read, R.J. *J. Appl. Cryst.* **2007**, *40*, 658-674.

36. Emsley, P.; Lohkamp, B.; Scott, W.G.; Cowtan, K. *Acta Cryst. Sect. D* **2010**, *66*, 486-501.

Highlights

- Inhibition of soluble epoxide hydrolase can offer therapy for in many diseases
- A novel spirocyclic diamine scaffold was explored in the design of sEH inhibitors
- Low nanomolar lead inhibitor was identified which is chiral and non-racemic
- The lead compound is distinctly polar, water-soluble and orally bioavailable
- Crystal structure of the lead inhibitor with sEH was obtained

Graphical abstract

Discovery of Polar Spirocyclic Orally Bioavailable Urea Inhibitors of Soluble Epoxide Hydrolase

Alexey Lukin, Jan Kramer, Markus Hartmann, Lilia Weizel, Victor Hernandez-Olmos, Konstantin Falahati, Irene Burghardt, Natalia Kalinchenkova, Darya Bagnyukova, Nikolay Zhurilo, Jarkko Rautio, Markus Forsberg, Jouni Ihanainen, Seppo Auriola, Jukka Leppänen, Igor Konstantinov, Denys Pogoryelov, Ewgenij Proschak, Dmitry Dar'in and Mikhail Krasavin[*]

sEH IC_{50} = 4.99 nM
Kinetic PB solubility >0.5 mM
$LogD_{7.4}$ = 0.99